

UCSF

UC San Francisco Electronic Theses and Dissertations

Title

Chemoreceptor Feedback by the Unfolded Protein Response

Permalink

<https://escholarship.org/uc/item/0z78b1sw>

Author

Dalton, Ryan P

Publication Date

2015

Peer reviewed|Thesis/dissertation

Chemoreceptor Feedback by the Unfolded Protein Response

by

Ryan Dalton

DISSERTATION

Submitted in partial satisfaction of the requirements for the degree of

DOCTOR OF PHILOSOPHY

in

Neuroscience



in the

GRADUATE DIVISION

Abstract

Each olfactory sensory neuron (OSN) expresses exactly one olfactory receptor (OR) gene, a feature which requires both a limiting or inefficient process of OR transcriptional activation and a subsequent process of OR feedback. Monogenic expression of ORs is thought to underlie the ability of animals to sensitively and specifically identify innumerable cues, and therefore understanding how olfactory receptor genes are transcriptionally activated and how they elicit feedback are problems of paramount importance in understanding the development of the olfactory system. The thesis project presented herein demonstrates that OR feedback is elicited through a surprising ability of olfactory receptor protein to elicit the unfolded protein response (UPR), a ubiquitous and highly-conserved proteostatic signaling pathway that is typically thought to be responsive to stress conditions. Activation of the UPR by OR expression in OSNs drives translation of a transcription factor specific to chemosensory neurons, resulting in stabilization of OR choice and monogenic OR expression, OSN maturation, and a termination of further OR choice. This signaling pathway is general to vomeronasal sensory neurons (VSNs) and is most likely also found in other sensory cells with limited patterns of G protein-coupled receptor expression including neurons of the trigeminal ganglion and the taste receptor cells of the tongue. Finally, the means by which ORs and vomeronasal receptors (VRs) activate the UPR is shown, with ORs and VRs activating the UPR indirectly and directly, respectively. Thus, while these receptors have divergent mechanisms of UPR activation, they have a convergent use of the UPR in order to coordinate monogenic receptor expression and to time development to the appearance of the chemoreceptor.

Table of Contents

A. Background	1
1. Introduction to the Murine Olfactory System	1
2. OR, TAAR, and VR Patterns of Expression	4
3. An Outline of OR Choice	5
a. Initial Constraints	6
b. Transcriptional Activation	6
c. Enhancer Elements	6
d. Epigenetic Regulation	7
4. An Outline of OR Feedback	7
a. Serizawa et al. 2003	8
b. Lewcock & Reed 2004	8
c. Shykind et al. 2004	8
d. Lyons et al. 2013	8
5. OR and VR Production and Trafficking	9
6. The Unfolded Protein Response	11
B. Hypothesis and Experimental Rationale	12
C. MOE Results	13
1. Atf5 is Required for OR Feedback	13
2. OR Expression Regulates Atf5 Translation	15
3. Control of Atf5 Translation	17
4. Unfolded Proteins Act as a Developmental Signal in OSNs	19

5. ORs do not Strongly Bind to PERK	20
6. ORs Activate PERK Through a Failure to Exit the ER	21
7. Persistent UPR Destabilizes Cell Fate and Prevents OSN Maturation	23
8. An Atf5-independent Cell Lineage	24
9. Cyclic AMP Control of Atf5 Transcriptional Activity	25
10. Atf5 Binds to OR Enhancer Elements	26
11. A Possible Role in OR Feedback for Cebpg	27
D. VNO Data	28
1. Lsd1 and Atf5 Actions in the VNO	28
2. Mechanism of PERK Activation by VRs	29
E. Discussion	30
1. A Multi-Part Model for OR Feedback	31
2. A Model for VR Feedback	32
3. Convergences and Divergences in Chemosensory Receptor Feedback	32
4. A Model for Stochastic TAAR Choice	34
5. An Atf5-Independent Cell Lineage	35
6. cAMP, Atf5 Activity, and OR Enhancers	36
7. Final Notes and the Naked ER	37
F. Methods	38
1. Immunohistochemistry	38
2. qPCR	39
3. RNAseq	42
4. Peptide array	43

5. Fluorescence Anisotropy	43
6. Transgenic mouse lines	44
7. Luciferase assays	44
8. Electrophoretic mobility shift assays	45
9. Tunicamycin injection	47
G. Figures	48
H. References	72
I. Library Release	84

List of Figures

Figure 1: RNAseq in <i>Atf5</i> mutant and control MOE.	48
Figure 2: ADCY3 and LSD1 IHC in <i>Atf5</i> mutant and control MOE.	49
Figure 3: Lineage tracing in <i>Atf5</i> mutant and control MOE.	50
Figure 4: <i>Atf5</i> expression in wt MOE.	51
Figure 5: ATF5 IHC in <i>Lsd1</i> mutant and control MOE.	52
Figure 6: ADCY3 and ATF5 expression in <i>Eif2S51A</i> mutant and control MOE.	53
Figure 7: ADCY3 and ATF5 expression in <i>Perk</i> mutant and control MOE.	54
Figure 8: ADCY3 and ATF5 expression with tunicamycin.	55
Figure 9: Olfr1507 and PERK cLD peptide array.	56
Figure 10: ATF5 expression in <i>Rtp1</i> transgenic MOE.	57
Figure 11: TAAR expression in <i>Atf5</i> transgenic MOE.	58
Figure 12: Gene switching in <i>Atf5</i> transgenic MOE.	59
Figure 13: OR expression in <i>Atf5</i> mutant MOE.	60
Figure 14: Luciferase expression with <i>Atf5</i> fusion constructs.	61
Figure 15: EMSA assay with enhancer probe.	62
Figure 16: OR expression in <i>Cebpg</i> mutant and control MOE.	63
Figure 17: ATF5 and CLGN expression in <i>Cebpg</i> mutant and control MOE.	64
Figure 18: ATF5 expression in <i>Cebpg</i> mutant and control VNO.	65
Figure 19: VR and CLGN expression in <i>Lsd1</i> mutant and control VNO.	66
Figure 20: ATF5 expression in feedback mutant VNO.	67
Figure 21: CLGN expression in wild-type MOE and VNO.	68
Figure 22: CLGN expression in feedback mutant VNO.	69

Figure 23: V1rb2 and PERK cLD peptide array.	70
Figure 24: Fluorescence anisotropy with V1rb2 and Olfr1507 probes	71

A. Background

1. Introduction to the murine olfactory system

Olfaction is mediated by olfactory sensory neurons (OSNs) located in the main olfactory epithelium (MOE) and vomeronasal sensory neurons (VSNs) located in the vomeronasal organ (VNO). Herein, the main topic of study is the MOE and OSNs, but information on the VNO and associated cells and receptors will be given when required for understanding of data presented. OSNs and VSNs send axons to the olfactory bulb, with the precise area of innervation depending both on the subfamily of chemoreceptor and the specific receptor within that subfamily that is expressed (Barnea et al. 2004, Bozza et al. 2009, Ebrahimi & Chess 2000, Johnson et al. 2012, Mombaerts et al. 1996, Ressler, Sullivan, & Buck 1994, Vassar, Ngai, & Axel 1993, Wang et al. 1998, Feinstein et al. 2004). The MOE is neurogenic and pseudostratified, with stem-like cells located in the basal area and OSNs developing along a basal to apical axis, with mature OSNs most apical and extending dendrites past non-neuronal sustentacular cells and into the nasal airway.

Following commitment to the neuronal lineage, OSNs mutually-exclusively express one of at least two types of cell surface G protein-coupled receptors (GPCRs): olfactory receptors (ORs) (Buck and Axel 1991), trace amine-associated receptors (TAARs) (Liberles and Buck 2006, Johnson et al. 2012).

These receptors both determine the pattern of connection to the brain for each OSN (Barnea et al. 2004, Bozza et al. 2009, Ebrahimi & Chess 2000, Johnson et al. 2012, Mombaerts et al. 1996 and others) and determine the OSN receptive field (Araneda, Kini, & Firestein 2000), and are therefore considered to be central to sensory neuronal identity. The primary signaling pathway activated by ligand binding to ORs or TAARs results in activation of adenylyl cyclase III (ADCY3) and neuronal depolarization (Levy NS, Bakalyar HA, Reed RR 1991, Jones et al. 1990).

The mouse OR family is the largest known gene family, encoding some 1430 members, roughly 1075 of which are intact with the rest encoding pseudogenes. ORs are located in clusters throughout the mouse genome, being found on all chromosomes except the Y. Each OR gene is encoded by a single exon. ORs can be divided into two groups: the 160 evolutionarily more ancient, fish-like 'type I ORs', and the 1270 mammal-specific 'type II ORs' (Sullivan et al. 1996, Zhang & Firestein 2002, Clowney et al. 2011). The ligands for ORs have not been comprehensively mapped owing to a number of difficulties, some of which will be discussed in the **OR Feedback** section of the background material. Those with demonstrated ligands have variable sensitivity to a number of ligands, and likewise any given volatile molecule may act as a ligand on a number of different receptors (Araneda, Kini, and Firestein 2000). By and large it is thought that ORs are activated by ligands which do not elicit

hardwired behavioral responses, instead requiring an associative stimulus to gain meaning or valence.

OR pseudogenes, an important part of the studies presented herein, are highly variable, with many lacking start or stop codons and others lacking key functional domains (Serizawa et al. 2003). For the purposes of the present study, an OR pseudogene is any OR which is not expressed stably, a concept to be discussed later in the **OR Feedback** section of the background material. The relationship of this functional definition to the presence or absence of specific promoter, gene, or protein features of a given OR is at present not entirely described.

The TAAR family, which will be discussed only briefly herein, encodes some 15 members in a single genomic cluster, of which 14 are intact. TAAR expressing cells likely constitute an olfactory subsystem, as they are thought to be activated by aversive or attractive odorants to elicit hardwired behavioral responses (Liberles & Buck 2006, Ferrero et al. 2011, Ferrero et al. 2012).

The vomeronasal organ, located above the roof of the mouth in mice, is thought to mostly be responsible for detection of pheromones (Dulac & Axel 1995). It houses vomeronasal sensory neurons and their progenitors, with immature neurons and progenitors being found at the tissue margins (Halpern 1987). The vomeronasal organ expresses at least two chemoreceptor gene families:

the vomeronasal receptors (VRs) (Dulac & Axel 1995) and the formyl peptide receptors (Liberles et al. 2009, Riviere et al. 2009), the latter of which will not be considered herein.

The VR genes can be broken into two families with distinct evolutionary histories and distinct protein and gene structures. The type I VRs (V1Rs), expressed by the apically-located type I VSNs, are encoded by about 300 genes, ~150 of which are pseudogenes. V1Rs, like ORs, are encoded by single exons, and have a similar basic protein structure. These receptors are thought to be activated by volatile pheromones (Berghard & Buck 1996, Ryba & Tirindelli 1997, Del Punta et al. 2002). Type II VRs (V2Rs) are expressed by basal type II VSNs and are encoded by 280 total genes, of which 122 are intact. They are multi-exon genes, and the encoded proteins have long N-terminal extensions not observed on TAARs, ORs, or type I VRs.

2. OR, TAAR, and VR Patterns of Expression

The most striking feature of the murine olfactory system and the feature most considered herein is that from the enormous OR gene family, each OSN only expresses a single gene, and that OR gene only from a single allele (Chess et al. 1994, Ebrahimi & Chess 2000, Serizawa et al. 2003, Vassalli et al. 2002, Shykind et al. 2004). While perhaps only single-cell RNAseq experiments could definitively prove this 'one neuron, one receptor' rule, exhaustive multicolor

RNA in situ hybridization studies performed by many laboratories support the rule and it is considered as a given herein. TAARs are also expressed monogenically and monoallelically, but by OSNs not expressing ORs. A given OR is expressed in a restricted area of the MOE. While it was at first thought that there were only four of these areas, or 'zones' (Vassar, Ngai, & Axel 1993), it now seems more likely that there are in fact many zones, with each expressing a subset of the genomically-encoded ORs (Miyamichi et al. 2005). Thus, each OSN has only a subset of ORs that it can express, dictated by the location of the OSN within the MOE.

The case with VSNs and VRs is somewhat different. While gene-targeting experiments have shown that V1Rs are monogenically and monoallelically expressed by type I VSNs (Rodriguez et al. 1999), V2R expression is more complicated. The V2R genes can be broken into A, B, C, and D families. Each type II VSN expresses an A, B, or D family member and a single gene from the C family, in combinations that appear to be non-random (Martini et al. 2001, Ishii & Mombaerts 2011). Type II VSNs can be divided further, with the more basal cells also expressing at least one non-classical MHC gene from the *H2-Mv* gene family (Ishii et al. 2003, Ishii & Mombaerts 2008, Ishii & Mombaerts 2011, Loconto et al. 2003, Leinders-Zufall et al. 2014). The significance of this coexpression is not well-understood.

3. An Outline of OR Choice

The means by which ORs are expressed monogenically and monoallelically are the main interests of the Lomvardas laboratory. In order for an OR to be expressed monogenically, it must first be transcriptionally activated, a process we refer to as 'choice'. Subsequently, it must elicit feedback, which will be discussed below. In this section, an outline of the OR choice process is given.

a. **Initial Constraints:** As discussed above, each OR gene is expressed in a distinct zone of the MOE, and this feature indicates initial constraints on OR choice (Vassar, Ngai, and Axel 1993, Ressler et al. 1994, Miyamichi et al. 2005, Lane et al. 2002, Michaloski et al. 2006). Swapping coding sequences of receptors from different zones results in swapping of zones in which these receptors are expressed, indicating that features surrounding the OR coding sequence most likely impart zonality (Wang et al. 1998).

b. **Transcriptional Activation:** OR promoter analysis indicates that most ORs share promoter features such as transcription factor binding sites. These features include O/E-like sites (Lane et al. 2002, Michaloski et al. 2006, Clowney et al. 2011, Plessy et al. 2012). OR promoters are also enriched for homeodomain sites, and two homeodomain proteins, LHX2 and EMX2, have been shown to regulate OR expression (Hirota & Mombaerts 2004, Hirota et al. 2007, Levi et al. 2003, McIntyre et al. 2008).

c. **Enhancer Elements:** Several enhancer elements have been demonstrated to be required for OR expression. The first of these identified, termed 'H'

(Lomvardas et al. 2006), is required in cis for expression of a handful of nearby ORs (Fuss, Omura, and Mombaerts 2007). Subsequently a number of other enhancers has been discovered. While a functional role has not yet been demonstrated for all of these enhancers, intriguingly they are found to congregate on the active OR allele, indicating that monogenic choice could be executed by the rare event of congregation of many trans enhancer elements (Lomvardas et al. 2006, Markenscoff-Papadimitriou et al. 2014, Fuss, Omura, & Mombaerts 2007).

d. **Epigenetic Regulation:** Chromatin immunoprecipitation (ChIP)

studies have demonstrated that the entire OR family is coated with repressive chromatin modifications such as trimethylation of histone 3, lysine 9 (H3K9me3) and trimethylation of histone 4, lysine 20 (H4K20me3) (Magklara et al. 2011). These marks are deposited prior to and independent of OR choice. Because OR genes are silenced prior to choice, it follows that their transcriptional activation requires chromatin modification. One enzyme has been identified to be required for this process, the lysine-specific demethylase *Lsd1*. LSD1 is expressed in immature OSNs during OR choice and is downregulated in mature OSNs, and loss of this enzyme almost entirely abolishes OR choice (Lyons et al. 2013, Lyons et al. 2014).

4. An Outline of OR Feedback

In addition to a limiting or inefficient process of OR choice, monogenic OR expression requires a subsequent process of OR feedback. The existence of

OR feedback was indicated by several studies, and these studies formed the foundation of this thesis project.

- a. OSNs that choose a deleted OR gene from a YAC transgene or that select an OR gene with a naturally-occurring frameshift mutation select a second receptor gene (Serizawa et al. 2003), indicating both that the OR gene suppresses further choice and that this suppression is specific to the OR.
- b. Deletion of the start codon of the OR also allows OSNs choosing this allele to select another OR gene (Lewcock & Reed 2004). This study indicated that intact OR protein is required to elicit OR feedback.
- c. OSNs choosing a deleted OR not only select a second OR allele for expression, but also suppress the expression of the first-chosen allele. In addition, a small minority of cells choosing an intact OR gene switch this gene off and choose another (Shykind et al. 2004). This process is known as 'gene switching', and it indicates that OR feedback acts to stabilize expression of the chosen OR gene.
- d. Deletion of *Lsd1* and subsequent loss of OR expression prevents expression of *Adcy3*, and *Adcy3* is required to terminate OR choice via downregulation of *Lsd1*. Rescue of OR expression also rescues *Adcy3* expression (Lyons et al. 2013). This study demonstrates that the OR is required and sufficient for *Adcy3* expression, that *Adcy3* terminates OR

choice, and that the crucial link in the feedback process is the connection between OR appearance and *Adcy3* expression.

The studies outlined above together support a model for OR feedback in which this pathway has several functions. OR feedback acts to promote *Adcy3* expression and OSN maturation, to terminate OR choice via LSD1 downregulation, and to stabilize expression of the chosen OR gene. In addition, because only certain ORs and not others activate OR feedback, for an OR to be expressed stably, it must pass some measure of protein quality control, and OR feedback therefore can be thought to select against the expression of OR pseudogenes. At the time that this thesis project was undertaken the molecular mechanisms of OR feedback had not been demonstrated.

5. OR and VR Production and Trafficking

ORs, like all other secretory and transmembrane proteins, are translated at the endoplasmic reticulum (ER). ORs are 7-transmembrane-pass proteins (Mombaerts 1999), over 90% of which have a single positionally stereotyped far N-terminal N-glycosylation site (our unpublished results). Mutation of this N-glycosylation site appears to destabilize OR choice (Feinstein et al. 2004), which offered initial support to a model in which OR structural elements were important in OR feedback.

It has been widely demonstrated that ORs and VRs fail to traffick to the plasma membrane when expressed heterologously (for example, Saito et al. 2004, Dey & Matsunami 2011). Failure to traffick of ORs in heterologous systems appears to be due to the lack of required specific chaperones or transporters. Many of these factors are sufficient to promote cell surface expression when coexpressed with ORs in cell lines, including receptor transporting proteins 1 and 2 (RTP1 and RTP2) (Saito et al. 2004), RTP1S (Wu et al. 2012), and HSC70T (Neuhaus et al. 2006). Because of the large size of the OR family, it is likely that different ORs require different chaperones or transporters for cell surface expression. Importantly for this work, the best-characterized of these molecules are RTP1 and RTP2, and these molecules are not expressed in OSNs at appreciable levels during OR choice. Therefore, ORs are expressed into a 'naked' ER that lacks molecules to endow an ability to traffick ORs.

VRs also fail to exit the ER when expressed heterologously. However, this appears to be due to a different regulatory principle. When *Calreticulin* (*Calr*), a ubiquitous soluble ER-luminal chaperone, is depleted from cell lines, VRs can traffick to the cell surface, as CALR appears to strongly bind VRs. Interestingly (and relevant to further discussion below), *Calr* depletion also reduces VR activation of the unfolded protein response in cell lines. CALR is absent in VSNs, allowing VR trafficking in these cells. It is replaced by a related protein that is VSN-specific, *Calreticulin 4*. (Dey & Matsunami 2011). Thus, ORs and VRs appear to employ different principles in their trafficking, with ORs requiring

specific factors for transport and VRs requiring the absence of ubiquitous chaperones.

6. The Unfolded Protein Response

As the precise folded shape of a given protein determines its function, it stands to reason that disruptions to protein shape could give rise either to loss of function or to gain of new function. Cells therefore have developed a means by which to monitor the folding state of their proteome. Secretory and transmembrane proteins are monitored in the ER lumen. Unfolded proteins, directly or through aggregation/sequestration of chaperones, activate ER-luminal sensors to trigger a signaling pathway termed the Unfolded Protein Response (UPR) (Ron & Walter 2007). Activation of this pathway, which is homeostatic in nature, acts to both increase the protein folding capacity of the ER and to decrease the rate of new translation initiation. The latter is executed by the ER-resident sensor PERK, which following sensing of unfolded proteins becomes activated and acts as an EIF2a kinase, resulting in an attenuation of protein translation through limitation of initiator tRNA (Ron & Walter 2007). For the purposes of this project, the most important feature of PERK is that it appears to bind directly to unfolded proteins, with those proteins acting as PERK-activating ligands (unpublished results).

Paradoxically, phosphorylation of EIF2a also results in the translational induction of a small set of mRNAs, the best characterized of which is *Atf4* (Vattem & Wek 2004). These genes contain two important features that allow this. First, they have small upstream open reading frames (uORFs), which following translation allow ribosomes to reinitiate translation at downstream ORFs. Second, they contain an inhibitory uORF (iuORF) that overlaps the main coding sequence (CDS) out of frame. During basal translation conditions, this iuORF is translated, but EIF2a phosphorylation results in skipping of the iuORF and translation of the CDS (Ron & Walter 2007). The mRNAs translated under these conditions are for the most part stress-responsive, as their protein only appears under conditions of stress.

C. Hypothesis and Experimental Rationale

The purpose of this project was to identify the molecular mechanism by which OR protein activates OR feedback to drive *Adcy3* expression. Given the extraordinarily large size of the OR family and a considerable diversity in OR primary sequence, it appeared that the most reasonable model to explain OR feedback would have OR signaling playing a dominant role. However, deletion of the G protein interaction site on the OR (a 'DRY' to 'RDY' mutation) does not preclude monogenic OR expression or lead to loss of stability of OR expression (Imai et al. 2006), indicating that at least in initial stages of OR feedback, OR signaling is not required.

Supporting this assertion (though see dicussion section), as noted above *Adcy3* is

itself a target of OR feedback, and thus canonical OR signaling cannot be performed until the OR has elicited feedback. We instead hypothesized that OR protein could generate the feedback signal by activating the unfolded protein response. If this were the case, then we would expect either that canonical components of the UPR would be repurposed in the MOE (for example through use of different transcriptional targets) or that non-canonical UPR components would be found specifically in the MOE. Through extensive searching of RNA in situ hybridization atlases, we identified activating transcription factor 5 (*Atf5*) (as a promising candidate gene (Hansen et al. 2002)). The majority of results presented below pertain to the function of *Atf5* in OR feedback. However, results also include experiments aimed at uncovering mechanisms of UPR activation by various chemoreceptors, as well as initial studies on transcription factors that may cooperate with *Atf5*. These results are split into two sections: one section on findings in the MOE and one on findings in the VNO. In the discussion section, the convergences and divergences in these results are examined.

D. MOE Results

1. *Atf5* is Required for OR Feedback

If *Atf5* is required for OR feedback, then upon *Atf5* deletion, the following should be observed: (a) OR choice should remain intact; (b) OR choice should no longer drive *Adcy3* expression; (c) OR choice should no longer result in

downregulation of *Lsd1* expression; and (d) OR choice should be destabilized. Using a commercially-acquired *Atf5* mutant mouse line, we assayed OR choice. In wild-type and mutant animals, whole MOE was used to isolate RNA, build cDNA libraries, and perform RNAseq experiments. As shown in **Figure 1**, OR choice is intact in *Atf5* mutant animals. While the average expression value of detected ORs is decreased in *Atf5* mutants relative to wild-type animals, nearly the same number of OR species are detected in mutants as in control animals, indicating that OR choice is intact. The decreased level of expression can be explained by subsequent findings.

Using immunohistochemistry (IHC), we next asked whether subsequent to OR choice, OSNs express the OR signaling molecule *Adcy3*. As shown in **Figure 2**, deletion of *Atf5* results in a near-total loss of ADCY3-expressing mature OSNs (mOSNs) compared to a wild-type control animal. Furthermore, the persisting mOSNs have an intriguing regular spatial distribution, indicating perhaps that these persisting cells constitute a distinct OSN subtype, a question addressed later in this work. In addition to the loss of ADCY3 expression, *Atf5* mutants show a clear expansion of LSD1 immunoreactivity. Whereas in control animals, LSD1 is restricted to the most basal area of the MOE, where OR choice is taking place, in *Atf5* mutants, LSD1 can be found across the entire thickness of the MOE (**Figure 2**).

Finally, we assayed the stability of OR expression in *Atf5* mutants. To perform this experiment, we took advantage of two mouse lines: the MOR28iCre line, in which Cre recombinase is expressed from an internal ribosome entry site (IRES) downstream of the endogenous MOR28 (*Olf1507*) locus; and a line harboring a flox-stop-flox-tomato cassette at the *Rosa26* locus. Thus, in animals harboring both of these alleles, any cell that has chosen MOR28 will be indelibly marked with tomato. We can therefore ask later, using a MOR28 antibody, whether tomato-marked cells (ie cells that have chosen MOR28) continue to express MOR28. MOR28 is an intact OR gene and previous studies have shown anywhere between ~1% (Shykind et al. 2004) and ~30% (Lyons et al. 2013) gene switching from this allele. Crossing these alleles into the *Atf5* mutant background and assaying for MOR28 transcriptional stability, we found a drastic defect. While in wild-type animals roughly 70% of cells that have chosen MOR28iCre (ie are marked with tomato) continue to express MOR28 by immunofluorescence, in *Atf5* mutant animals only around 10% of MOR28iCre-choosing cells continue to express this receptor. Thus, stability of an intact OR allele is disrupted by deletion of *Atf5* (**Figure 3**)

Together, these data indicate that OR feedback is deficient in *Atf5* mutant animals: OR choice proceeds, but fails to drive *Adcy3* expression, fails to downregulate LSD1, and fails to promote OR transcriptional stability.

2. OR Expression Regulates *Atf5* Translation

The finding that *Atf5* is required for OR feedback does not answer the central question of this thesis project, namely how ORs are detected in the first place. However, given that *Atf5* is required for *Adcy3* expression and that OR expression is required and sufficient for *Adcy3* expression, the problem is reduced to how OR expression controls *Atf5* expression. To begin to answer this question, we first characterized the expression pattern of *Atf5* in more detail. To do this, used RNAseq libraries from three cell populations in the MOE: Intercellular adhesion molecule 1+ cells (*Icam1*+, which marks horizontal basal cells, stem cells at the basal margin of the MOE), Neurogenin 1+ cells (*Ngn1*, which marks neuronal progenitors at around the time of OR choice (Cau et al. 1997)), and olfactory marker protein+ cells (OMP, which marks mature OSNs). As seen in **Figure 4**, *Atf5* mRNA is highly abundant in each of these cell types, typically expressed at a higher level than highly-abundant housekeeping genes. We next assayed the pattern of ATF5 protein expression. As seen in **Figure 4**, by IHC ATF5 protein is found in a highly restricted region of the MOE corresponding to immature OSNs. Intriguingly, ATF5 protein appears at around the developmental stage at which OR expression is initiated, and disappears just prior to expression of ADCY3.

This pattern of ATF5 protein expression was remarkable for two reasons. First, it placed ATF5 protein between OR expression and ADCY3 expression, supporting its role in OR feedback. But more importantly, it suggested that *Atf5*

translation could be regulated by OR expression. To test this, we assayed ATF5 protein expression in *Lsd1* mutant and control animals. *Lsd1* mutants do not express ORs, as noted above. Compared to wild-type animals, *Lsd1* mutants have a drastic reduction in ATF5 protein expression, although *Atf5* mRNA remains essentially unaffected (**Figure 5**). Thus, OR expression is required for translation of *Atf5*. To test whether OR expression was sufficient to drive *Atf5* translation, we employed a rescue strategy. In the *Lsd1* mutant background, we expressed an OR transgene with the G protein gamma 8 (*Gng8*) driver (*Gng8-tta*). As seen in **Figure 5**, rescue of OR expression in the *Lsd1* mutant background also rescues *Atf5* translation, indicating that OR expression is sufficient to drive *Atf5* translation.

3. Control of *Atf5* Translation

The *Atf5* mRNA structure is unusual, containing features only observed in other UPR- or integrated stress response-regulated transcripts. Most importantly, *Atf5* contains an uORF that is out-of-frame with the reading frame of the CDS. During basal conditions, this uORF is translated, inhibiting translation of the *Atf5* CDS. For this reason, it is referred to as an inhibitory iuORF. Translation of the CDS in genes that contain an iuORF typically follows phosphorylation of the translation initiation factor EIF2a. This phosphorylation event acts to slow assembly of translation-competent ribosomes, resulting in ribosome scanning to downstream ORFs. It has been previously demonstrated that *Atf5* translation follows EIF2a phosphorylation (Watatani et al. 2008). To

test whether EIF2a phosphorylation is required for translation of *Atf5* in OSNs, we assayed ATF5 protein expression by IHC in animals in which the EIF2a phosphorylation site is mutated, rendering EIF2a active regardless of regulation (*eif2S51A*). In homozygous *eif2S51A* animals, ATF5 protein is totally absent, and ADCY3+ neurons are not observed, despite *Atf5* mRNA abundance remaining high (**Figure 6**).

There are four mammalian EIF2a kinases, each responding to a unique cellular stress such as double-stranded RNA, heme depletion, or appearance of unfolded proteins. The unfolded protein-regulated kinase is PERK, which has an ER-luminal sensing domain and cytoplasmic-facing kinase domain. To test whether PERK was required for phosphorylation of EIF2a, we assayed ATF5 protein expression by IHC in homozygous *Perk* mutant animals. As shown in **Figure 7**, and ATF5 protein expression is absent in *Perk* mutant animals despite robust *Atf5* mRNA, and ADCY3+ neurons are not observed. These findings indicate that the ability of ORs to drive *Atf5* translation is due to activation of PERK and EIF2a phosphorylation.

Finally, it may be possible that the developmental defect seen in *eif2S51A* and *Perk* mutants is not due to loss of ATF5 expression, but instead due to loss of other factors that are uniquely translated under these conditions. To test this, I generated an *Atf5* transgene lacking the *Atf5* translational control elements and under the control of the tetracycline transactivator protein (tta). By expressing

this transgene under the control of the *Gng8* promoter driving *tta* (*Gng8-tta*), it is thus possible to express ATF5 protein during the developmental window in which it would normally occur. When the *Atf5* transgene is expressed in *EIF2S51A* mutant animals, ADCY3 expression is rescued (**Figure 6**). These results indicate that the developmental defect seen in *EIF2S51A* and *Perk* mutant animals is due to loss of ATF5.

4. Unfolded Proteins Act as a Developmental Signal in OSNs

The finding that PERK is activated by OR expression to drive *Atf5* translation was unusual, given that PERK activation typically occurs downstream of cellular stresses, acting to homeostatically maintain cellular proteostasis. This finding suggested a model in which ORs somehow act like unfolded proteins to activate PERK. To test whether the appearance of unfolded proteins was indeed the feedback signal in the MOE, we performed a genetic/pharmacological experiment. Heterozygous *Lsd1* animals were incrossed. When pregnant females reached the E16 stage for their carried pups, they received a single intraperitoneal injection of the drug tunicamycin, which drives general protein misfolding and UPR activation through blocking protein N-glycosylation in the ER. *Lsd1* mutant and wild-type pups were harvested at E17 and assayed for ATF5 and ADCY3 expression by IHC. As seen in **Figure 8**, injection of tunicamycin in *Lsd1* mutant animals not only entirely rescues ATF5 translation, but to a limited degree rescues ADCY3 expression as

well. We speculate that the inability of tunicamycin to drive a full ADCY3 rescue is due to the fact that OSNs in this condition have compromised protein translation initiation. Thus, the presence of unfolded proteins in the developing OSN ER lumen is sufficient to elicit OR feedback, indicating that the appearance of unfolded proteins is indeed the feedback signal.

5. ORs do not Strongly Bind to PERK

PERK activation by OR expression could occur either via direct binding, as has been demonstrated for another UPR sensor, IRE1 and the unfolded protein substrate Carboxypeptidase Y (CPY*). Alternatively, the ability of ORs to activate PERK could stem from the inability of ORs to traffick from the ER, resulting in general protein misfolding, perhaps through sequestration of chaperones.

In order to discriminate between these two models, we first performed biochemical experiments to map PERK-OR interactions. Peptide arrays were generated on which OR amino acid primary sequences were used to generate overlapping 18-mer peptides in 3 amino acid steps. For example, the first position on the membrane corresponds to amino acids 1-18 of an OR, the second spot corresponds to amino acids 4-21, and so on. Peptides from the entire OR sequence were bound to a membrane, and the ligand-binding region of PERK (core luminal domain, cLD), fused to Glutathione-S-transferase (GST)

was washed over the membrane. GST enzymatic activity was then used to identify OR-derived peptides to which PERK cLD was bound. The relative binding of each spot was averaged with its immediate upstream and downstream neighbors. As seen in **Figure 9**, several regions of the OR act to strongly bind PERK. However, as the PERK cLD is located in the ER lumen, only regions of the OR that would be ER-luminal are relevant to this analysis, with transmembrane or cytoplasmic regions lacking an opportunity to bind to PERK. When analysis is restricted to ER-luminal OR peptides, no regions are identified which strongly bind to PERK, suggesting that ORs do not act as direct PERK ligands.

6. ORs Activate PERK Through a Failure to Exit the ER

Given that ORs do not appear to strongly bind PERK, it may be more likely that PERK is activated through a failure of ORs to traffick from the ER. Indeed, it has been demonstrated by several groups that when ORs are expressed in heterologous systems, they fail to traffick from the ER, as discussed above. While both RTP1 and RTP2 have been shown to be sufficient to promote ER exit of OR protein, these results must be carefully considered however, as it is unlikely that RTP proteins can promote trafficking of the entire OR family, and unpublished results have at the least demonstrated heterogeneity in whether or not RTP proteins can promote ER exit of ORs. RTP1 has been shown to be a

direct target of ATF5 by ChIP-seq, indicating that once OR expression drives *Atf5* translation, ATF5 resolves UPR by driving *Rtp1* expression.

Because, as described above, RTP1 expression is sufficient for the ER exit of some ORs, loading the ER with RTP1 prior to or coincident with OR choice should allow ORs to exit from the ER immediately. Therefore, ORs should experience no failure to traffick and should not sequester chaperones to drive general protein misfolding. To test this model, we generated another tta-regulated transgenic mouse line, in which tta regulates expression of *Rtp1* and *Rtp2*. By crossing this transgenic line to the *Gng8-tta* line, the ER will be loaded with RTP1 and RTP2 coincident with OR choice (as opposed to following feedback). As seen in **Figure 10**, early expression of RTP1 and RTP2 both shifts ATF5 immunoreactivity apically and decreases the level of OMP expression by qPCR. Furthermore, if the *Rtp1/Rtp2* transgene is expressed under the control of both *Gng8-tta* and *OMP-tta*, giving it persistent expression across OSN development, ATF5 immunoreactivity is almost entirely absent (**Figure 10**). These data support a model in which OR expression is only sufficient to drive ATF5 translation under conditions in which ORs fail to exit the ER. As an important control, we also assayed maturation of VSNs in these same animals. If RTP1/RTP2 are specific to ORs, then early RTP1/RTP2 expression in the VNO should not prevent VSN maturation. As shown in **Figure 10**, *Rtp* transgenic MOE but not VNO have a defect in maturation, supporting this hypothesis.

7. Persistent UPR Destabilizes Cell Fate and Prevents OSN Maturation

The finding that ATF5 translation is context dependent, occurring only in the absence of RTP1, prompted us to ask whether the relief of UPR and ATF5 translation is itself a developmental signal. Some ORs may be sufficient to drive ATF5 translation but could then fail to exit the ER through failure to interact with RTP1, resulting in prolonged ATF5 translation and a failure of the OR to traffick productively to the cell surface. In this situation it would be beneficial for OSNs to undergo gene switching to express an OR that could contribute to olfaction. To test this idea, we expressed the ATF5 transgene discussed in section D3 under the control of both Gng8-tta and OMP-tta, giving rise to a MOE in which ATF5 is expressed for a longer period than endogenous ATF5. To assay development, we both examined sections of the MOE by IHC and performed RNAseq. As seen in **Figure 11**, persistent ATF5 expression results in an almost complete loss of ADCY3 expression. In addition, we performed lineage tracing experiments identical to those described in section D1. These experiments showed that prolonged ATF5 expression also destabilizes cell fate (**Figure 12**). Thus, in addition to ATF5 appearance acting to control OSN development, ATF5 disappearance acts as a molecular cue. Our RNAseq analysis (**Figure 11**) and subsequent IHC experiments revealed that the types of receptors expressed by OSNs changed dramatically, with the most drastic increase seen in TAAR expression in transgenic animals. Finally, many cells

were observed in which multiple TAARs are expressed (**Figure 12**). A speculative model to account for this increase in TAAR expression is presented in the discussion.

8. An *Atf5*-independent Cell Lineage

Given that prolonged ATF5 expression results in destabilization of cell fate, we also asked whether failure to translate ATF5 results in an enrichment of alternate cell fates. As shown in **Figure 2**, mOSNs are observed in ATF5 mutants, albeit at greatly reduced numbers. We hypothesized that these persisting cells may represent a lineage that does not use receptor-mediated feedback to develop. This lineage may be present in the MOE but invisible in most experiments, as it would be expected to express many of the same markers as other mOSNs but perhaps with a different receptor complement. To ascertain the identity of these cells, we crossed the *Atf5* mutant mouse line to one in which OMP drives GFP expression. *Atf5*^{-/-}; *OMP-GFP* animals had MOEs dissected and used for FACS. Sorted cells had RNA isolated and used for RNAseq. RNAseq data was compared to OMP-GFP data from *Atf5* heterozygous animals prepared concurrently. As seen in **Figure 13**, a number of ORs are highly overrepresented in the *Atf5* mutant dataset. A cursory analysis revealed that these ORs are highly-unusual, containing additional N-glycosylation sites (ORs have a highly-stereotyped single N-glycosylation site) (data not shown). In addition, at least two of the most highly-represented OR species, *Olfir856-ps1*

and *Olf1372-ps1*, are pseudogenes that are *Lsd1*-independent (data not shown). In addition to overrepresentation of these OR species, canonical OR signaling molecules are expressed at greatly reduced levels in these OSNs compared to wild-type OSNs. Most notably, the soluble guanylate cyclase *Gucy1b2* (*GCS-beta-2*) is highly overrepresented (**Figure 13**), indicating that these persisting cells may employ both different receptors and a different signaling pathway from most OSNs. Thus, this GUCY1B2+ cell type may develop along with mOSNs, becoming visible only in the absence of other mOSNs. The significance of *Gucy1b2* expression will be examined in the discussion.

9. Cyclic AMP Control of ATF5 Transcriptional Activity

Like some other bZip transcription factors, ATF5 transcriptional activity could be regulated by cyclic AMP (cAMP). If this were the case, then appearance of cAMP at OSN maturation would change the function of Atf5. If this changed function were to the detriment of the maturation program of the cell, then it would be advantageous for Atf5 protein to only appear briefly to activate expression of target genes such as *Adcy3*, which could provide another reason that UPR control of *Atf5* translation could be advantageous. ATF5 protein expression in the mOSN context could in theory then modulate or inactivate expression of genes activated by ATF5.

To test whether ATF5 activity is regulated by cAMP, we cloned chimeric *Atf5* constructs in which the ATF5 activation domain was fused to the DNA-binding domain of the Tet Repressor Protein (tetR). We then transfected this '*Atf5s*' construct into HEK293 cells along with a tet-responsive luciferase construct. Following transfection, lysates were harvested and used for luciferase assay. As seen in **Figure 14**, in the absence of cAMP, this construct robustly activates luciferase transcription, but in the presence of forskolin, which stimulates adenylyl cyclases to generate cAMP, the *Atf5-tetR* construct had no transcriptional activity (compare to the tetR DNA-binding domain alone). As a control, we also used an *Atf5* construct in which the CDS is from a different reading frame. This construct had no activity in transgenic assays but maintains DNA binding properties ('*Atf5L*', data not shown and **Figure 15**). Thus, it appears that ATF5 transcriptional activity can be controlled by cAMP. The significance of this finding will be discussed below.

10. Atf5 Binds to OR Enhancer Elements

While we demonstrated above that *Atf5* is required for stabilization of OR expression, our published results do not provide any mechanism for this. One hypothesis is that ATF5 directly regulates OR enhancers, such that the activity of an enhancer is modified when ATF5 protein is produced downstream of OR expression. To test whether ATF5 binds to OR enhancers, we performed electrophoretic mobility shift assays (EMSAs) using probes derived from

putative ATF5 binding sites on OR enhancers suggested by DNA footprinting analysis, and *Atf5*-transfected or mock-transfected HEK293 cell nuclear lysate. As can be seen in **Figure 15**, an OR enhancer-derived DNA probe shows equivalent mobility shifts in the presence of *Atf5*-transfected nuclear lysate but not in the presence of control nuclear lysate. These results indicate that ATF5 does indeed bind to at least one OR enhancer. Unfortunately, ATF5 ChIP experiments failed, preventing any comprehensive analysis of ATF5 binding. However, these results along with results from section D9 lend support to a model to be discussed later.

11. A Possible Role in OR Feedback for *Cebpg*

Given that ATF5 protein is expressed in many tissues and that it is a bZip family transcription factor, specificity in ATF5 regulatory activity may be due to coexpression of different ATF5-binding proteins in different tissues. One factor known from in vitro assays to bind to ATF5 is the CCAAT-enhancer binding protein gamma (*Cebpg*). Interestingly, DNA footprinting analysis performed in our lab also identified binding sites for CEBPG on OR enhancers, suggesting that ATF5 and CEBPG could act in concert to regulate these elements. To test whether CEBPG has a role in OR feedback, we performed IHC and RNAseq analysis on *Cebpg* knockout and control whole MOE. As seen in **Figure 16**, OR expression is intact in *Cebpg* knockout animals; however, while these animals display robust *Atf5* translation, ATF5 protein fails to enter the

nucleus. Consequently, no OSN maturation is observed. As a control, we examined ATF5 protein expression in the VNO on these same sections, and found that in the VNO, ATF5 protein is nuclear, though VSNs also fail to mature (**Figure 18** and data not shown). *Atf5* transfections in HEK cells yield robust nuclear ATF5, regardless of *Cebpg* coexpression (data not shown). In contrast to *Atf5* mutant animals, in which limited OSN maturation is seen (discussed above), nearly no mOSNs were observed in *Cebpg* knockouts. These data indicate that the persisting cells in *Atf5* knockout animals develop in a context that requires CEBPG but not ATF5, a finding to be discussed later. Full RNAseq data for *Cebpg* knockouts can be found in.

E. VNO Data

1. LSD1 and ATF5 Actions in the VNO

Given our findings in the MOE, an obvious next question was whether the receptor-mediated feedback pathway identified in the MOE was widespread. We first tested this in the VNO. As shown in **Figure 19**, loss of *Lsd1* from the VNO prevents expression of V1Rs as assayed by IHC with an antibody that recognizes many type I VRs. As seen in **Figure 19**, loss of *Lsd1* also prevents VSN maturation. Thus, VR expression is required for VSN maturation.

We next tested whether in the VNO, as in the MOE, VR expression drives *Atf5* translation. As seen in **Figure 20**, loss of VR expression via *Lsd1* deletion prevents *Atf5* translation. Furthermore, *Atf5* translation is abolished in *Perk* and *eif2S51A* mutant mouse lines. Thus, VR expression drives *Atf5* translation through activation of PERK and phosphorylation of eif2a.

Finally, using RNAseq analysis, we identified the gene *Calmegin* as highly – enriched in mOSNs and mVSNs (**Figure 21**) and used a CALMEGIN antibody to assay for VSN maturation. As seen in **Figure 22**, loss of VR expression or *Atf5* translation result in a total loss in mVSNs. Thus, as is observed in the MOE, VR appearance in VSNs appears to drive *Atf5* translation and VSN maturation. It has been previously reported that VR expression, unlike OR expression, is stable (Roppolo et al. 2007). Therefore the function of ATF5 in the VNO may not include regulation of VR expression, though this has not yet been tested.

2. Mechanism of PERK Activation by VRs

As discussed above, OR activation of PERK is most likely indirect, occurring through a failure to traffick from the ER. In contrast to ORs, VRs can traffick to the cell surface in heterologous systems as long as the ubiquitous chaperone Calreticulin (*Calr*) is absent. *Calr* is absent in VSNs, presumably allowing for VR trafficking. To test whether VRs employ direct or indirect means to activate PERK, we again performed peptide array experiments as described in section

D5. Unlike ORs, two luminal regions of VRs were found to be very strong PERK binders (**Figure 23**). To corroborate these data, we performed fluorescence anisotropy experiments using tagged 18-mer peptides corresponding to the second and fourth ER-luminal regions of the VR. These experiments revealed that these peptides are extremely strong PERK binders, with a K_d of 7.603 μ M for the second ER-luminal region and 8.049 μ M for the fourth ER-luminal region. As a control, we also performed anisotropy experiments using an ER-luminal-derived OR peptide. This peptide did not show strong binding to PERK in these assays (**Figure 24**). Thus, PERK activation by VRs may be direct as opposed to indirect for ORs. If this is the case, then either VRs may continue to activate PERK throughout the lifetime of the VSN, or these regions may be shielded or otherwise prevented from activating PERK. Indeed, as PERK activation results in general reduction in protein translation initiation, and persistent PERK activation can result in apoptosis, persistent PERK activation by the VR would be an unusual strategy. Nonetheless, an examination of a wild-type adult VNO demonstrates that *Atf5* translation is persistent, occurring in most mature VSNs (**Figure 24**). Whether this represents pulses of *Atf5* translation or persistent translation and whether VSNs must have specific regulatory features that prevent induction of apoptosis are examined in the discussion.

F. Discussion

1. A Multi-Part Model for OR Feedback

The results presented above lend support to a model for OR feedback in which the key signaling event is the activation of PERK. Together, they indicate that upon OR expression, PERK is activated, driving phosphorylation of EIF2a, leading to *Atf5* translation. ATF5 then activates *Adcy3* transcription, which acts to terminate *Lsd1* expression.

ORs presumably must pass a number of quality control steps in order to become monogenically expressed in the MOE. First, ORs must activate the PERK branch of the UPR, either through a failure to traffick or otherwise. Next, ORs must be able to interact productively with RTP1 or other chaperones in order to exit the ER and reach the cell surface. Finally, it has recently been shown that G protein beta/gamma signaling is important in termination of OR choice in zebrafish (Ferreira et al. 2014). Thus, a final test may be a test of the ability of the chosen OR to signal through these proteins.

We have shown herein that failure to either activate UPR or relieve UPR both result a failure of OSNs to mature, to terminate OR choice, or to stabilize expression of the chosen receptor. Presumably, ability to activate the UPR ensures not only that a receptor has been chosen, but that it is expressed at appreciable levels, as it is easy to imagine that a receptor that fails to traffick but is expressed poorly at the protein level would fail to activate UPR. Ability of

the OR to relieve UPR subsequently would act as a filter to prevent termination of OR choice following 'bona fide' ER stress conditions. Finally, signaling through G proteins could act as a confirmation of OR identity.

2. A Model for VR Feedback

While V1R expression is monogenic, it does not share one key feature with OR expression, namely that when a VSN chooses a VR pseudogene, it does not extinguish expression of this gene, but instead continues choosing VRs. This results in coexpression of the VR pseudogene with an intact VR (and could in theory lead to expression of many VR pseudogenes in a single cell, a hypothesis yet to be tested). Given this feature, the primary role of ATF5 in the VNO may be to coordinate receptor appearance to VSN maturation and to terminate VR choice. We propose that, similar to the role of *Adcy3* and G protein beta/gamma in the MOE, ATF5 in the VNO activates expression of signaling molecules that act to terminate VR choice.

3. Convergences and Divergences in Chemosensory Receptor Feedback

The MOE and VNO are not the only tissues in which receptors are expressed in a monogenic or limited fashion or in which receptor expression acts to define cell identity. We therefore propose that a UPR-based feedback model could allow for stochastic cell fate acquisition in any tissue with these features. In

addition to our studies in the VNO and MOE, we have begun pilot studies in the trigeminal ganglion, where somatosensory neurons express several classes of chemoreceptors including genes from the Mrg family of receptors. We have also begun studies on the taste receptor cells of the tongue, which fall into one of several classes based on receptor expression. Importantly, the relationship between cell types in both of these tissues is unknown, and employing genetic strategies as roadblocks to neuronal diversification could clarify these relationships.

In the case of the VNO and MOE, it is intriguing that while receptor feedback systems converge on translation of *Atf5*, they arrive at PERK activation through apparently divergent mechanisms, with ORs appearing to activate PERK indirectly while VRs activate PERK directly. This convergence most likely reflects the utility of this pathway to achieve monogenic gene expression. However, the finding that UPR activation in the VNO is persistent is puzzling. Under conditions in which *Atf5* is translated, general protein translation initiation is attenuated, indicating that VSNs are most likely undergoing proteostatic stress throughout their life. In most cell types, failure to resolve UPR would eventually result in apoptosis, and it is therefore an intriguing possibility that VSNs have developed special anti-apoptotic signals that allow them to thrive despite frequent UPR activation. While IHC results show that UPR activation is widespread, a key caveat is that the kinetics of this system

are unclear, and UPR activation may be extremely transient but easy to visualize due to the high level of *Atf5* mRNA expression.

4. A Model for Stochastic TAAR Choice

TAAR+ cells are found throughout the MOE in a salt and pepper pattern that indicates that their choice could operate stochastically, similar to OR choice. However, TAAR gene bodies lack the epigenetic modifications of ORs, and these modifications have been demonstrated to be key in stochastic OR choice. Moreover, no TAAR enhancer elements have been identified despite analysis by this lab.

Given our results from *Atf5* transgenic animals with greatly expanded TAAR expression, it is very tempting to speculate that TAAR choice is driven by failure to relieve UPR, with ATF5 protein acting as the specific activating component. Importantly, in another genetic model in which *Atf5* translation is persistent, the *Adcy3*^{-/-} mouse, we also see an expansion in TAAR+ cells (data not shown). Thus, prolonged ATF5 protein expression may somehow directly influence TAAR choice. Prolonged ATF5 protein expression could be caused by selection of an OR that activates UPR but fails to interact with RTP1 or other chaperones to relieve UPR. Because the probability of choice of one of these receptors should be equal across OSNs, the probability that a cell will fail to

relieve UPR will also be equal, resulting in stochastic selection of TAAR genes. This model has yet to be tested directly.

5. An *Atf5*-Independent Cell Lineage

The finding that *Atf5* deletion prevents the majority of OSN maturation but allows for a small number of OSNs to persist was extremely intriguing. In particular, this finding was interesting because the persisting cells occur in a very regular and precise spatial orientation, indicating that these cells may use spatial cues in development. We set out to use the transcriptome of these cells as a window into their identity and eventually were able to obtain a single *Atf5* mutant mouse with the *OMP-GFP* allele. The most interesting finding from our RNAseq analysis of these cells is that they are greatly enriched for the soluble guanylate cyclase *Gucy1b2*. This is intriguing because it has been demonstrated recently that there is a subpopulation of OSNs that express *Trpc2* and *Gucy1b2*, with these cells presumably being sensitive to a different class of odors than other OSNs, possibly even pheromones. This possibility is especially exciting for selfish reasons. It is controversial whether humans can detect pheromones, as their VR family is entirely pseudogenized and the vomeronasal organ appears to be vestigial in humans. Thus, genetic and molecular evidence could come to bear if it is shown that a subset of ORs (those expressed in the *Gucy1b2*⁺ cells) act as pheromone receptors. This is of course entirely speculative, but certainly a worth course for future study.

Another interesting element of this part of the story is that these cells do not develop in the absence of *Cebpg*. This finding uncovers a branching point in the acquisition of OSN cell identity: cells that lack *Atf5* but have *Cebpg* can become this *Gucy1b2*⁺ class of cells, while those that lack both fail to acquire any mOSN fate. In addition to what has been demonstrated with our *Atf5* transgenes, this may indicate a fluid model of OSN cell fate acquisition, in which lack of *Atf5*, persistence of ATF5, or ATF5 in various contexts acts as a master regulator of acquisition of many classes of OSN cell fate. An alternative model for *Cebpg* activity is that it is a specific antiapoptotic molecule in OSNs and VSNs that prevents cell death during UPR activation, possibly only in the context of receptor expression. This possibility is an area of future study by the lab.

6. cAMP, *Atf5* Activity, and OR Enhancers

We demonstrated above that an OR enhancer element binds to ATF5 protein in biochemical studies. ATF5 binding sites are highly enriched on OR enhancers (Markenscoff-Papadimitriou et al. 2014). In addition, we have shown that ATF5 transcriptional activity is regulated by cAMP. These two findings together may be important pieces of the puzzle of OR choice and OR feedback. The strongest model would suggest that ATF5 acts to stabilize or assemble OR-enhancer contacts to promote robust OR transcription. If ATF5 were to persist into mOSN, cAMP would then inactivate the chosen OR gene. Alternatively, cAMP

could be the stabilizing element, converting ATF5 from a transcriptional activator to a structural element at enhancer-OR contacts. In essence, ATF5 and co-factors would act to identify OR enhancers early in OSN development, but would then hand these elements off to mature OSN transcriptional machinery. Supporting this model, a number of genes that require ATF5 for expression continue to be expressed in the absence of ATF5 in mOSNs.

7. Final Notes and the Naked ER

The UPR-based receptor feedback system identified by this project is important and warrants further study for a variety of reasons. First, it demonstrates an incredible coordination between different organelles in the establishment of cell fate. Second, it prompts a reevaluation of the core functionality of the UPR, which until these findings were published was thought to be mainly a homeostatic pathway. The fact that we have shown this pathway to be in widespread use in development indicates that this is not a minor function of the UPR, but instead one of its basic features. Third, this project should drive a reevaluation of ER homeostasis. The UPR, as described in the introduction to this work and in innumerable others, is described as restoring ER homeostasis through two specific functions: increasing the folding capacity of the ER and decreasing its protein folding load. Our studies demonstrate a restoration of ER homeostasis through specific tuning of the ER proteome- in some cases through addition of a single protein. This mode of

maintenance of homeostasis is qualitatively distinct and must be incorporated into models of ER and UPR function. Fourth, and most importantly, this project demonstrates how the appearance of a singularity (an OR, VR, etc.) could act to control the gene regulatory landscape of a cell. This is extremely important in consideration of the diversification of cell fates. Ultimately, if receptor choice is inefficient and the UPR is sensitive, then the number of cell identities that a tissue is capable of giving rise to is only limited by the number of genes in its sensory receptor gene family. Herein discussion is limited to chemoreceptors, but it is entirely feasible that any number of other receptors or other types of molecules could activate the UPR to drive cell fate diversification. For this to happen, these molecules could simply employ the system used by ORs. Specifically, any type of molecule that requires a specific chaperone or transporter could activate the UPR by being initially expressed into an ER environment which lacks that chaperone or transporter. Thus in a sense, the ER is kept 'naked', or denuded of specific protein elements, in order that the appearance of co-factors of those elements is endowed with an ability to control gene expression and cell fate acquisition.

G. Methods

1. Immunohistochemistry:

All sections shown were prepared as follows: whole MOE or VNO was dissected directly into OCT freezing medium; alternatively, tissue was fixed in 4% paraformaldehyde pH 7.2 in PBS (4% PFA) for 30 minutes, then washed briefly with PBS, then protected in 30% sucrose in PBS overnight. Sections were kept frozen. To prepare slides for use, they were thawed for at least 10 minutes at room temperature. Slides were fixed for 10 minutes with 4% PFA, then washed 3x5 minutes in PBS + .1% Triton-X (PBST), then blocked in PBST + 4% donkey serum for one hour at room temperature. Antibody was added in PBST + 4% donkey serum and sealed under a coverslip to incubate overnight at 4C. Coverslips were removed and slides were washed 3x15 minutes in PBST. All secondary antibodies were obtained from Invitrogen and used at 1:1000. Secondary antibodies were incubated on slides under coverslips for 1 hour at room temperature. Slides were then washed 3x15 minutes in PBST, briefly dried, and then mounted in vectashield. For DNA visualization, either DAPI or bis-benzimide were used. Primary antibodies used: Rabbit anti-MOR28 (gift from Gilad Barnea); goat anti-Atf5 (SC-46935) at 1:200; Rabbit anti-Adcy3 (SC-588) at 1:250, goat anti-Clgn (SC-133440), Rabbit anti-Lsd1 (ab17721). Imaging was performed on various Zeiss laser scanning confocal microscopes.

2. RT-qPCR

All qPCR data herein was generated by dissection of whole MOE or whole VNO into trizol (Invitrogen). RNA was isolated using the provided trizol protocol. 500ng DNase-digested total RNA was then used to generate cDNA, using superscript III (Invitrogen). cDNA was diluted 1:5 for qPCR. All primer sets used were 4.6uM stocks diluted 1:20. Reaction volumes of 20ul were used. Amplification was detected via SYBR incorporation in various Bio-Rad qPCR modules. The following primers were used:

gene				primer sequence
GAPDH_F				GGGTGTGAACCACGAGAAAT
GAPDH_R				CCTTCCACAATGCCAAAGTT
ActinB-F				GTCCACCTTCCAGCAGATGT
ActinB-R				GAAAGGGTGTAAAACGCAGC
Atf5-F				TGGCGACCCTGGGACTGGAG
Atf5-R				GGGCACCCCAAGGACCTCA
Lsd1-F				TGGGCCCGGGGCTCCTATTC
Lsd1-R				GGGGCCAGGAGTGATCGGCT
OMP-F				CGGGCACCTCGCAGAACTGG
OMP-R				CAGAAGATGGCGGCGGGGTC
Gap43-F				GATGCAGCCCCAGCCACCAG
Gap43-R				TCCGCTGAGCCGGCCTTTTC

vmn2r1-f				ATGCAGATTGATGGCCAAGT
vmn2r1-r				CACATGGGTGATACCGGCTC
vmn2r2-f				TGAGCCCAAAGAGCTAATGAC T
vmn2r2-r				CCCTTGCCTACATCTCCATTC A
vmn1r49-f				CCCCCAACTTGACCTCAGAAG
vmn1r49-r				TGGCCATAAGAGTGGAAAACC T
vmn1r8-f				TGTGCTGTGGCAAGTGTGTA
vmn1r8-r				CCCCACTGAGGCTATACAGAA C
T1R1-F				GCTTTCAGCTGCCAAAGGAC
T1R1-R				GAGGTCTGTGTCTCACCTGC
T1R3-F				GCCCCGAATAGTACCTCAGC
T1R3-R				AGGGTCCATCTTGTGCACTG
Calr4-F				GTTCTACGCCCTTTCCACCA
Calr4-R				CAATCGATGCCTTGCTCGTG
GalphaO- F				CTACGGGGCTGTGGACTCTA
GalphaO-				GGCTAGCCTCCAGGTTTTCTT

R				
Galphal2-F				CAGTGGACCTGGCAGGATG
Galphal2-R				GAGAATGAGCAGGTGGGCTT
Rtp1-F				TGCCCTGCCTTACACTTACC
Rtp1-R				CACTCACCTGTGGTCACACT
Vmn2r122f				TCACTGCTTGTCAGCAGGTTC
Vmn2r122r				AATCAAAGCAGCAATCTGCCG T
Vmn2r36f				TCTGGAAGTACCTGGACAGC
Vmn2r36r				ATGTGTCCTTTGGGGCCATC

3. RNAseq

RNA to be used for RNAseq was prepared as for qPCR. Following RNA isolation, Nugen ovation kits were used to prepare cDNA libraries for RNAseq. Sequencing was performed by elimbio or in house using the illumina platform. The bowtie/cufflinks/cuffnorm suite of programs was used to map reads and generate RPKM values.

4. Peptide arrays

Peptide arrays were generated by the MIT biopolymers laboratory. In short, Olfr151, Olfr1507, and V1rb2 primary sequences were tiled by 3 amino acids across their entire length to give rise to a set of overlapping 18-mer peptides. These peptides were bound to a nitrocellulose membrane. The membrane was incubated in methanol for 10 minutes, then binding buffer (50mM Tris pH 7, 250mM NaCl, 10% glycerol, 2mM DTT) for 3 10-minute washes. Arrays were then incubated with purified 500mM PERK cLD-GST fusion protein binding buffer. The arrays were then washed for 3x10 minutes to remove unbound cLD-GST. Bound cLD-GST was transferred to a PVDF membrane using a semi-dry transfer apparatus, and cLD-GST was then detected using anti-GST antibody from Abcam. To quantify binding intensity, signal for each spot was averaged with its immediate adjacent upstream or downstream neighboring spots. Data was normalized to the maximum binding intensity spot and plotted against amino acid position.

5. Fluorescence anisotropy

Peptides from the second and fourth ER-lumenal (ie extracellular) regions of V1rb2 were synthesized by New England Biolabs. The peptide sequences were: LKFKDCSVFYFVHIIMSHSYA and MFMPWGRWNSTTCQSLIYLHR. Both peptides had C-terminal FITC tags. Binding of labeled peptides was measured by the change in

fluorescence anisotropy on a Spectramax-M5 plate reader, with an excitation wavelength of 485nm and an emission wavelength of 525nm. Reaction volume was 20ul and 384-well black, flat-bottomed plates were used. All measurements were taken after a 30-minute incubation period. Anisotropy values were calculated as in Gardner & Walter 2011.

6. Transgenic mouse lines

All transgenic mouse lines generated used tta-inducible promoters. To generate these lines, *Atf5* or *Rtp1* were PCR amplified from MOE cDNA and subcloned using *EagI* and *EcoRV* sites into the pTre2 vector. Downstream from these insert genes was placed an internal ribosome entry site driving expression of enhanced GFP. These constructs were linearized and injected into a pronucleus of a fertilized one-cell host embryo. Embryos were then implanted. To determine whether transgenes were expressed, all animals with integration confirmed by PCR had MOE dissected to assay native GFP fluorescence. Only lines with the highest levels of expression were maintained.

7. Luciferase assays

The ATF5 activation domain was predicted using uniprot. This domain was cloned from cDNA and subcloned as a fusion with the tet repressor protein. This construct, as well as a tet-inducible luciferase construct, were co-transfected using

lipofectamine 2000 into HEK293 cells. 24 hours post-transfection, cells were scraped in luciferase buffer from promega, then collected and luciferase signal was detected in 96-well plates in triplicate using a Promega dual-luciferase assay system.

8. Electrophoretic mobility shift assays

HEK293 cells were transfected with pTre2-Atf5-IRES-GFP and a plasmid encoding tta or tta alone. 24 hours post transfection, GFP expression was confirmed using an epifluorescence microscope. Cells were trypsinized for 5 minutes. Trypsin was quenched with DMEM + 10% FBS. Cells were spun for 5' at 500g at 4C, and supernatant was aspirated. Cells were washed in hypotonic buffer (10mM HEPES pH 7.5, 60mM KCl, 1.5mM MgCl₂ and protease inhibitors), then pelleted. 3 pellet volumes of hypotonic buffer were added to cells and cells were swelled on ice for 10 minutes. Cells were lysed by gravity dounce on ice, then pelleted for 5 minutes at 1600g at 4C. Pellet was resuspended with ½ pellet volume hypotonic buffer, then an equivalent volume of hypertonic buffer (20mM HEPES pH 7.5, 1.2M KCl, 25% glycerol, 1.5mM MgCl₂, protease inhibitors) was added dropwise while pellet was gently vortexed. This mixture was incubated at 4C for 30 minutes on a rotisserie, then spun 20 minutes at 14000rpm at 4C. Supernatant was flash frozen on liquid nitrogen.

To generate probe, 25uM of each complementary synthesized oligos were boiled 5 minutes in annealing buffer (10mM Tris pH 7.5, 50mM NaCl, 1mM EDTA), then allowed to cool to <30C for 45 minutes to 1.5 hours. Annealed oligos were treated with 1ul exonuclease for 15 minutes at 37C, then purified with G50 columns and run on an agarose gel with unanneled probe to confirm annealing. To label probes, 25pmol dsDNA was incubated with polynucleotide kinase (and buffer) with 1ul g-ATP (150mCi/ml) for 30 minutes at 37C. Probe was purified with G50 columns and activity was quantified with scintillation counter.

Probes used:

Sfak2 footprint CACC	CACCCTGCCTTATATATTCTGTCTTGTGGTTCCTGG
	CCAGGAACCACAAGACAGAATATATAAGGCAGGGTG
lipsi footprint CACC	CACCAGATCATACTCTCGAAGGCAGACAAGTTAATT
	AATTA ACTTGTCTGCCTTCGAGAGTATGATCTGGTG

100000 cpm probe was incubated with 10ul nuclear extract for 20 minutes at RT. Mixture was then loaded on a polyacrylamide gel. Gel was run cool either in cold room or with cold pump. Gel was then transferred to whatman paper using a gel dryer, then incubated with a phosphoimager screen overnight and imaged the next day on a typhoon machine.

9. Tunicamycin injection

Lsd fl/fl females were crossed to Lsd fl/+; FoxG1-Cre males. 16 days after plug formation, females received a single intraperitoneal injection of 1ug tunicamycin in DMSO per gram body weight. One or two days later, animals were sacrificed and pups were embedded directly in OCT to prepare for immunofluorescence.

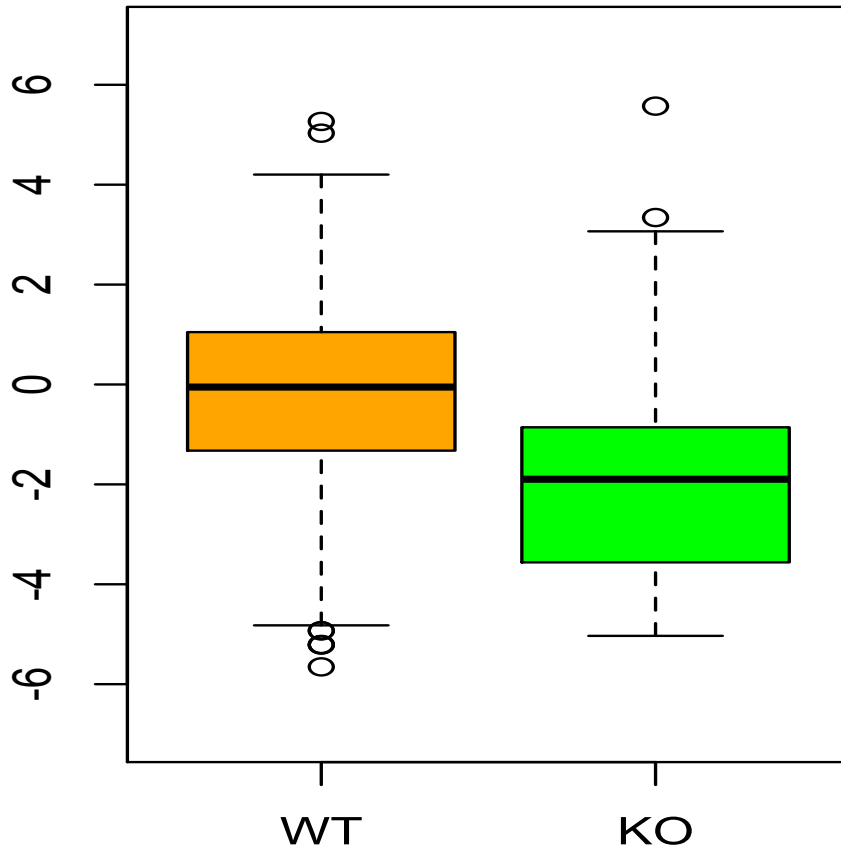


Figure 1: RNAseq analysis from whole P40 MOE RNA in Atf5 control and knockout animals. Data shown is for the OR gene family only, and is represented as log2(RPKM). Number of receptors detected per genotype is shown below figure. From Dalton, Lyons, and Lomvardas 2013.

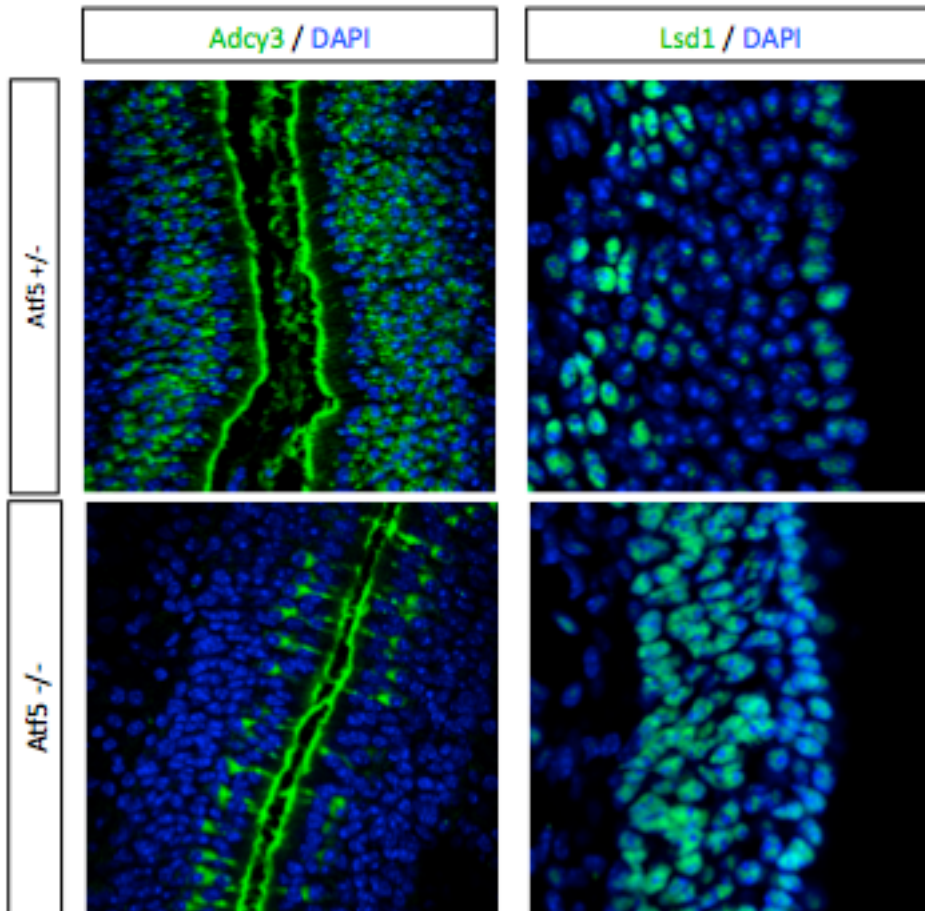


Figure 2: Adcy3 and Lsd1 protein expression in P40 Atf5 +/- and Atf5 -/- MOE coronal sections. From Dalton, Lyons, and Lomvardas 2013.

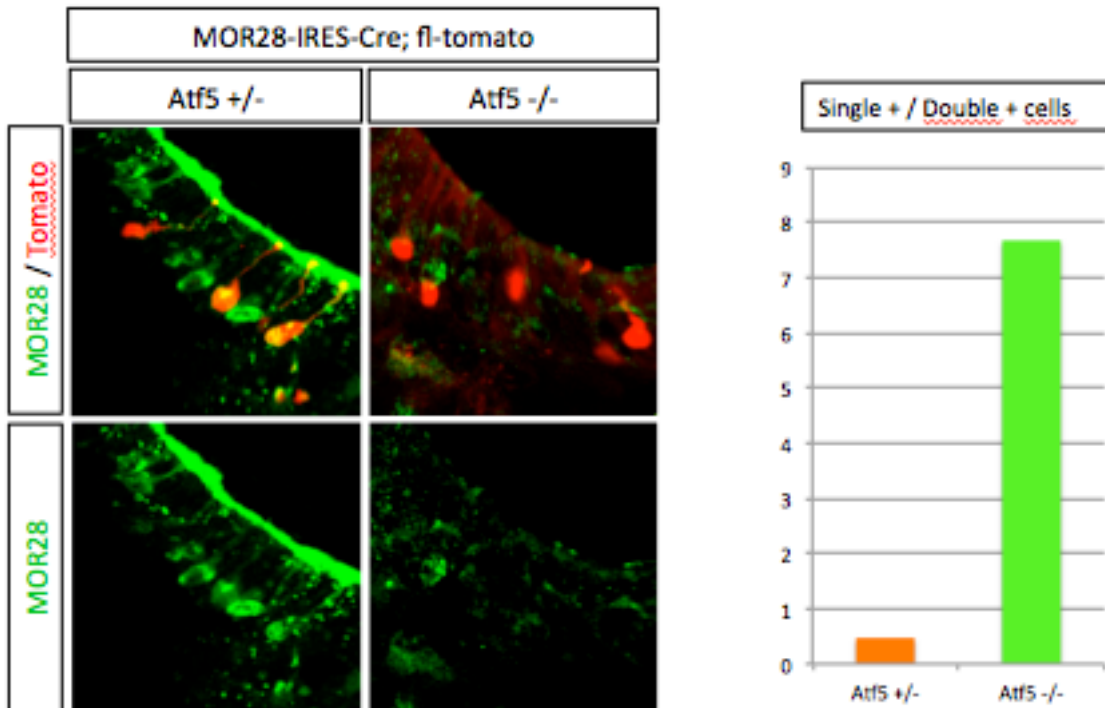


Figure 3: Left: lineage tracing analysis for MOR28-IRES-Cre in P40 Atf5 +/- and Atf5 -/- animals. Tomato+ cells have chosen MOR28 at some point in their lives. Right: data summarized, tomato+ cells / tomato+ and MOR28+ cells. From Dalton, Lyons, and Lomvardas 2013.

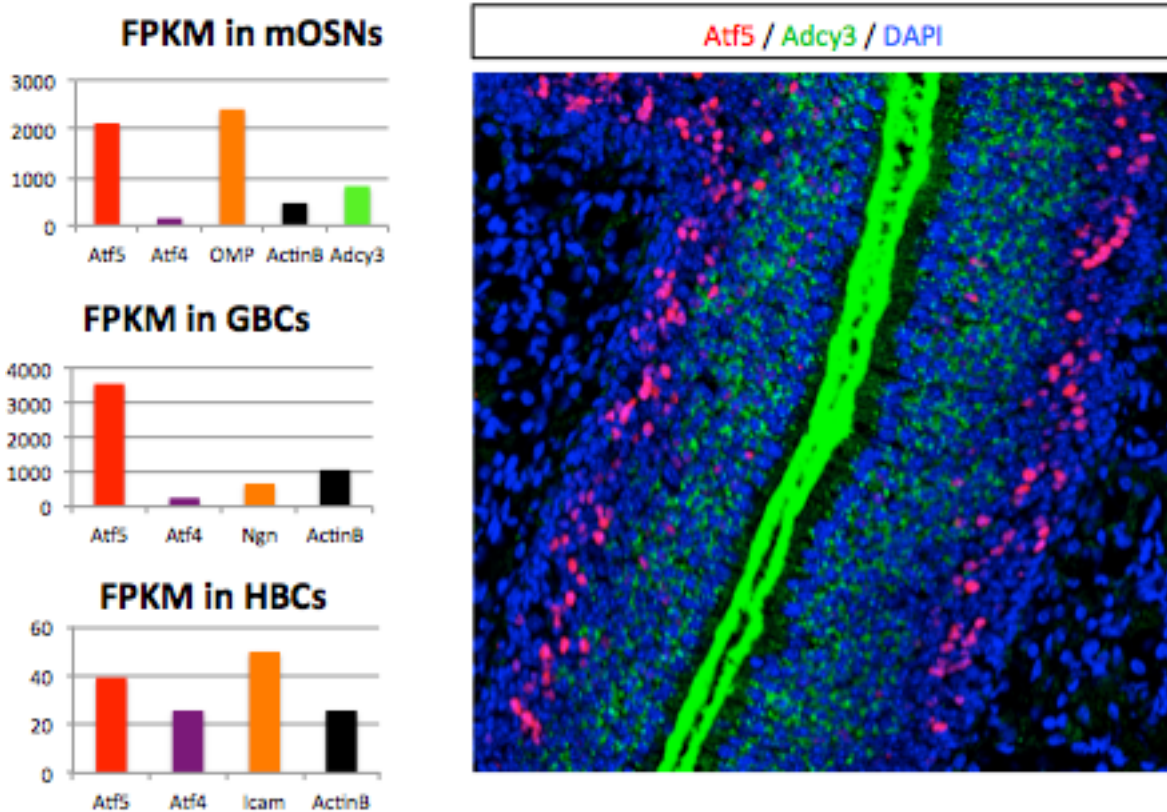


Figure 4: Left: Atf5 mRNA expression in horizontal basal cells, globose basal cells, and mature OSNs. Right: Atf5 and Adcy3 protein expression in a P40 coronal MOE section. From Dalton, Lyons, and Lomvardas 2013.

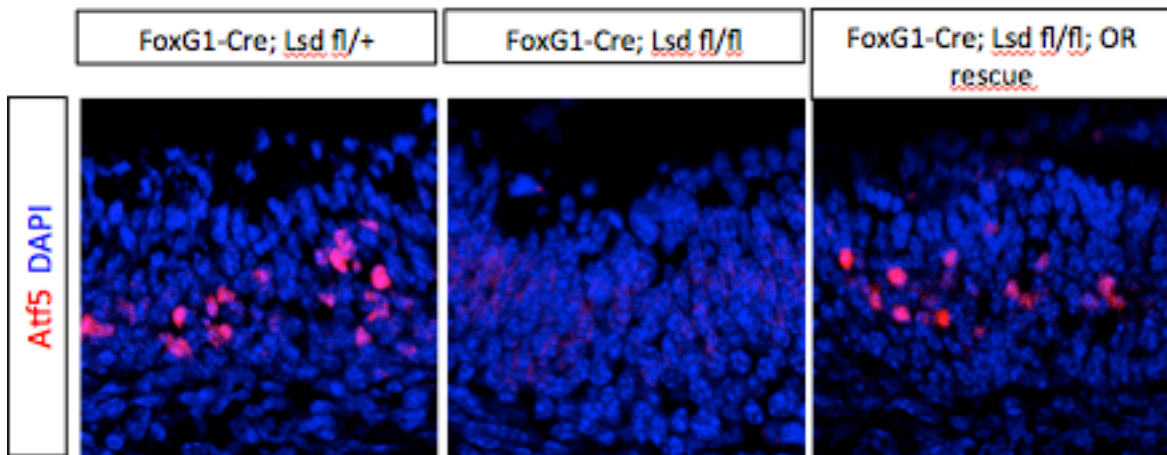


Figure 5: Atf5 protein expression in Lsd1 control, Lsd1 mutant, and Lsd1 mutant animals with transgenic OR rescue. From Dalton, Lyons, and Lomvardas 2013

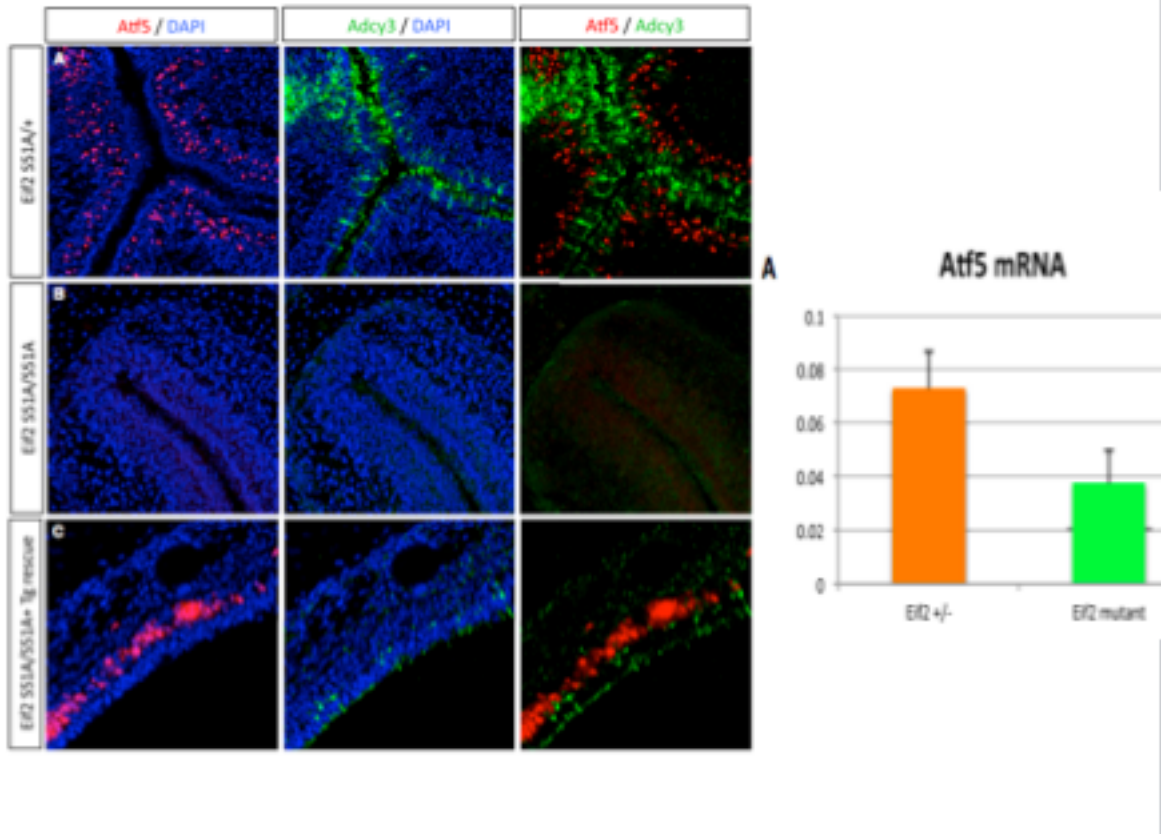


Figure 6: Left: Adcy3 and Atf5 protein expression in *Eif2S51A/+* and *Eif2S51A/S51A* littermates at PO. Right: Atf5 mRNA in these animals. Data shown is qPCR data on three animals per genotype. From Dalton, Lyons, and Lomvardas 2013.

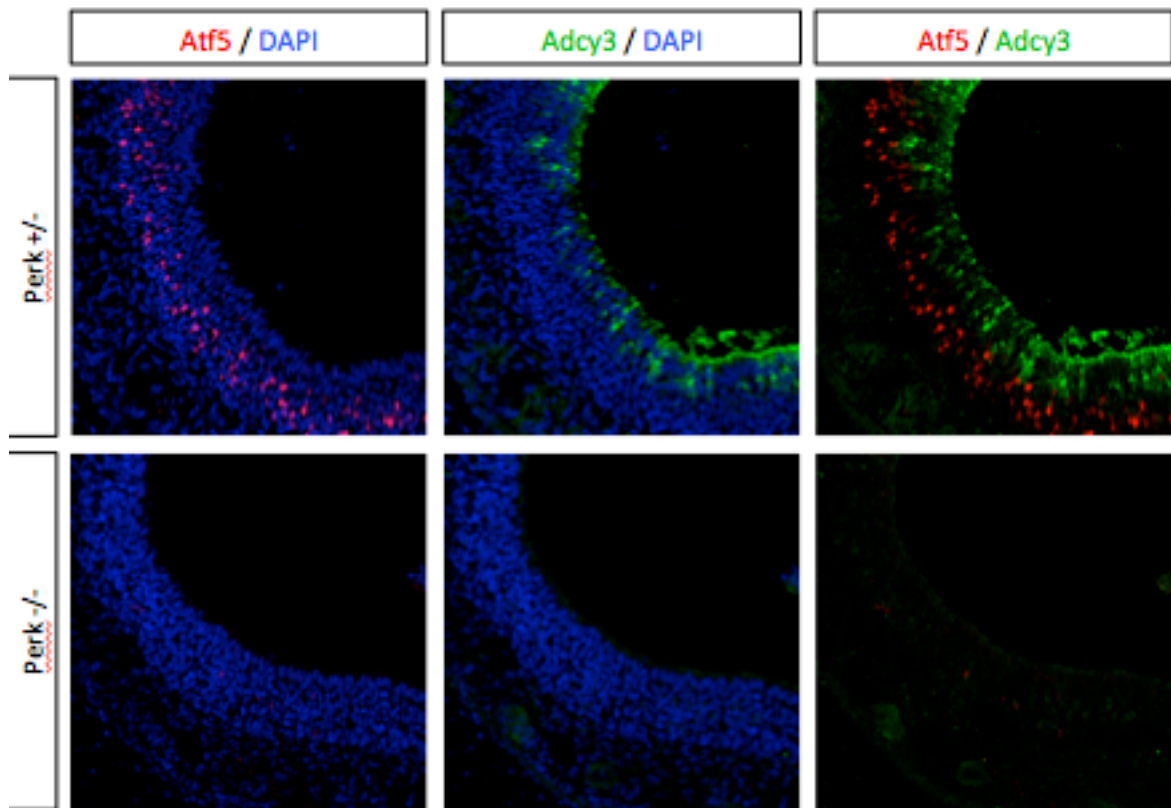


Figure 7: Atf5 and Adcy3 protein expression in *Perk +/-* and *Perk -/-* P0 littermates. From Dalton, Lyons, and Lomvardas 2013.

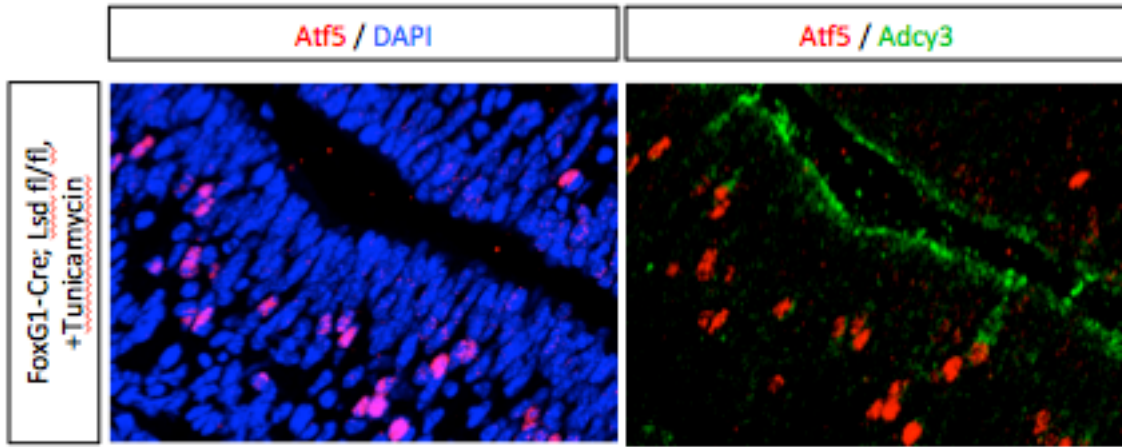
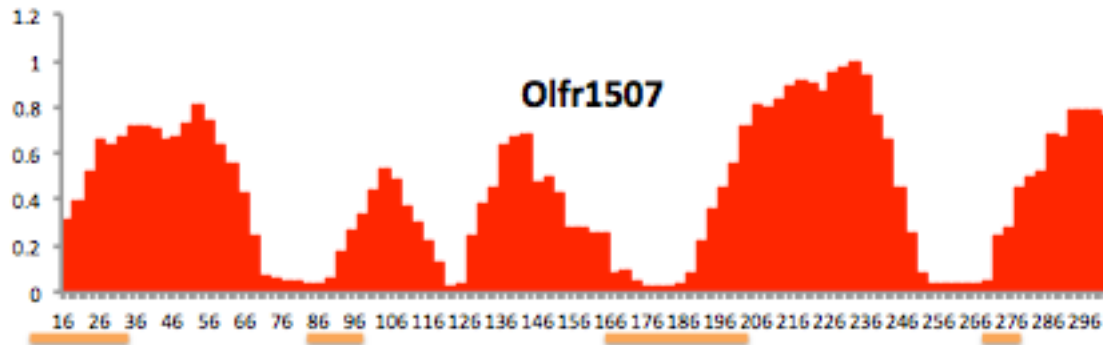


Figure 8: Atf5 and Adcy3 protein expression in Lsd1 mutant animals at E18 after a single tunicamycin injection at E16. Compare to figure 5. From Dalton, Lyons, and Lomvardas 2013.



ER-luminal regions.

Figure 9: Perk cLD binding to OR-derived peptides. Data shown as relative intensity versus amino acid position. ER-luminal regions are underlined in gold.

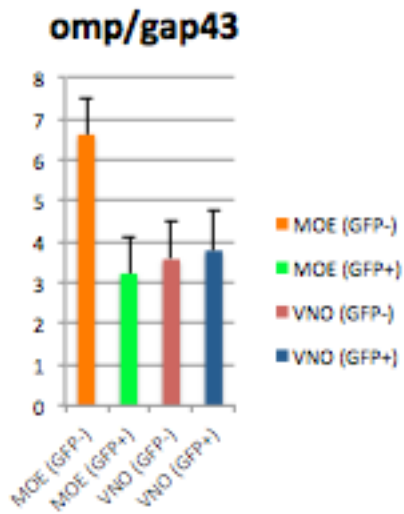
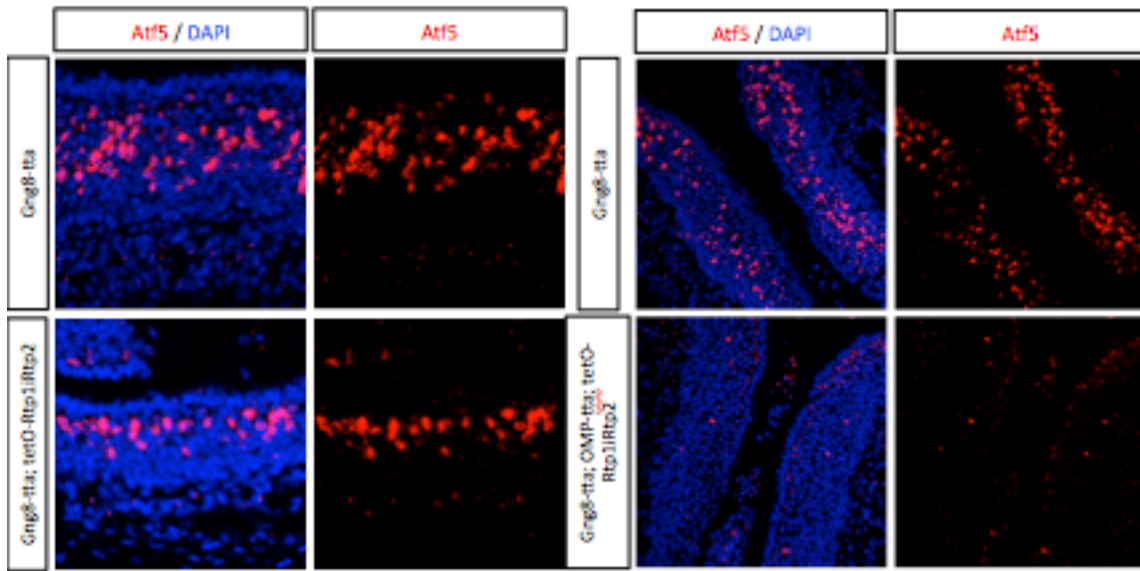


Figure 10: top: Atf5 protein expression in Rtp1/Rtp2 transgenic mice. Shown are sections from P21 mice expressing either Gng8-tta alone, Gng8-tta and the Rtp transgene, or Gng8-tta, OMP-tta, and the Rtp transgene. middle: OMP/Gap43 mRNA expression in Rtp1 transgenic animals with Gng8-tta alone versus control. Data shown are qPCR data from 3 animals per genotype and error bars represent standard error.

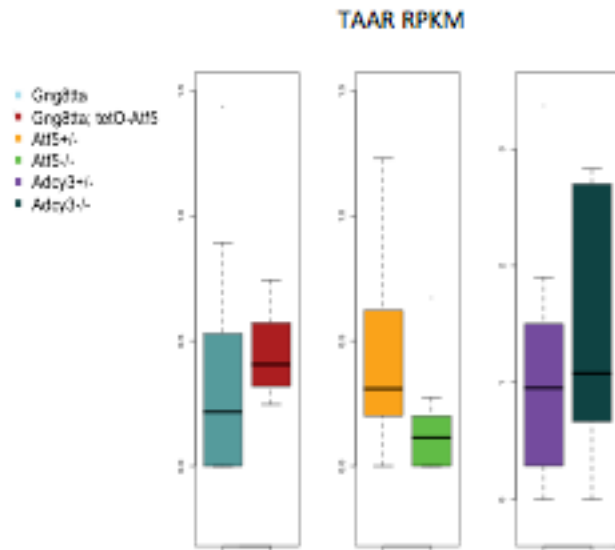
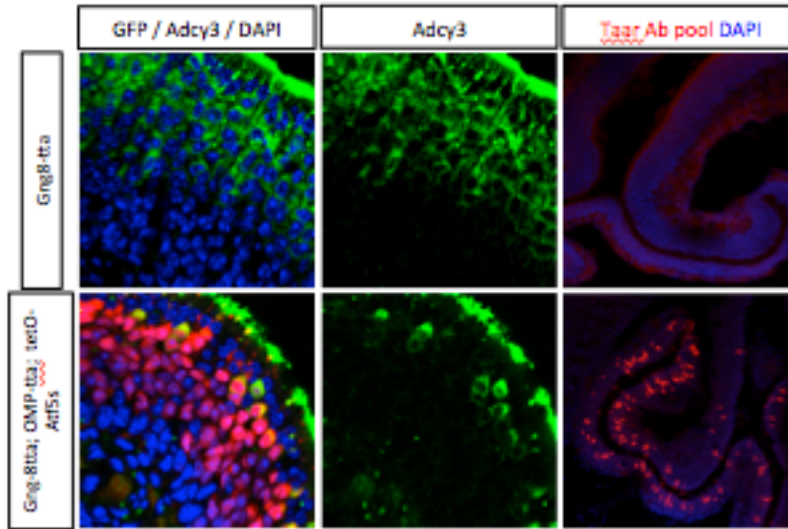


Figure 11: top: Atf5, GFP, Adcy3, and TAAR expression in control and Atf5 transgenic animals at P40. middle: RNAseq data for the TAAR gene family from genotypes indicated.

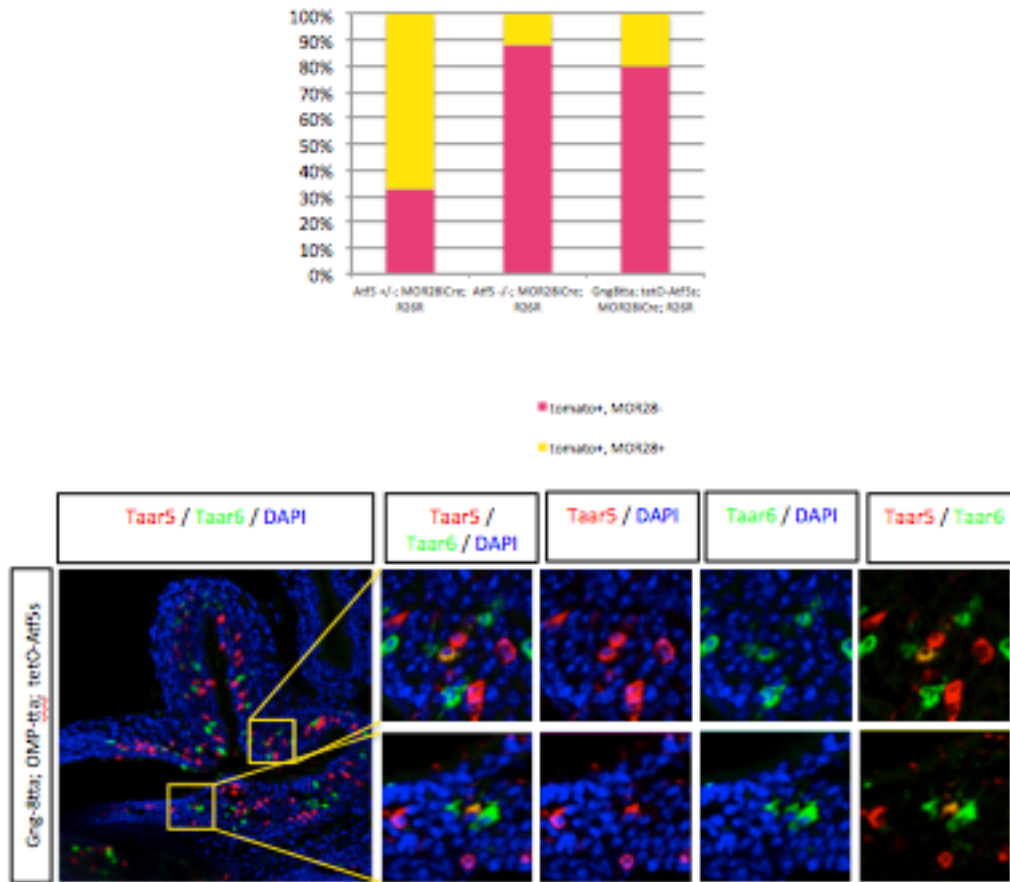


Figure 12: top: gene switching summary for Atf5 +/-, Atf5 -/-, and Atf5 +/- transgenic animals with Gng8-tta driver. Data represented as tomato+ cells versus tomato+/MOR28+ cells. middle: Atf5 transgenic animal with TAAR5 and TAAR6 protein labeled. Insets show coexpression of these genes.

Gene name	OMP-GFP RPKM	Atf5 -/-; OMP-GFP RPKM
Olf449	33.2612	452.852
Olf1383	40.0335	200.442
Olf856-ps1	7.50019	173.371
Olf309	5.73321	118.209
Olf124	34.2998	116.765
Olf1347	9.5877	89.7264
Olf2	21.1835	82.7848
Olf1348	38.761	80.3716
Olf1264	20.0662	68.7834
Olf372	1.27371	67.8161
Olf571	17.5927	66.8695
Olf592	22.5519	59.2994
Olf464	11.7385	43.5242
Olf24	5.61465	42.917
Olf15	38.761	39.4429
Olf129	17.0488	39.2931

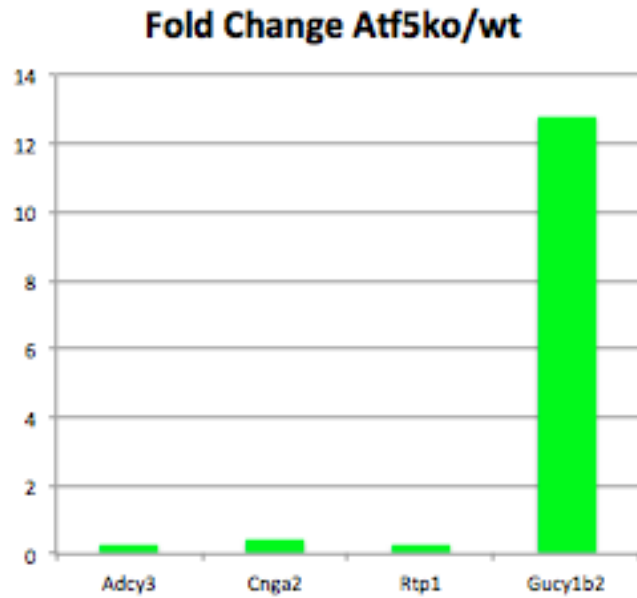


Figure 13: left: ORs overrepresented in FACS-isolated OMP-GFP+ cells from Atf5 -/- versus Atf5+/- . Data shown as RPKM. Right: fold change between Atf5-/- and Atf5 +/- from this same expression data for OR signaling molecules and the non-canonical signaling molecule Gucy1b2.

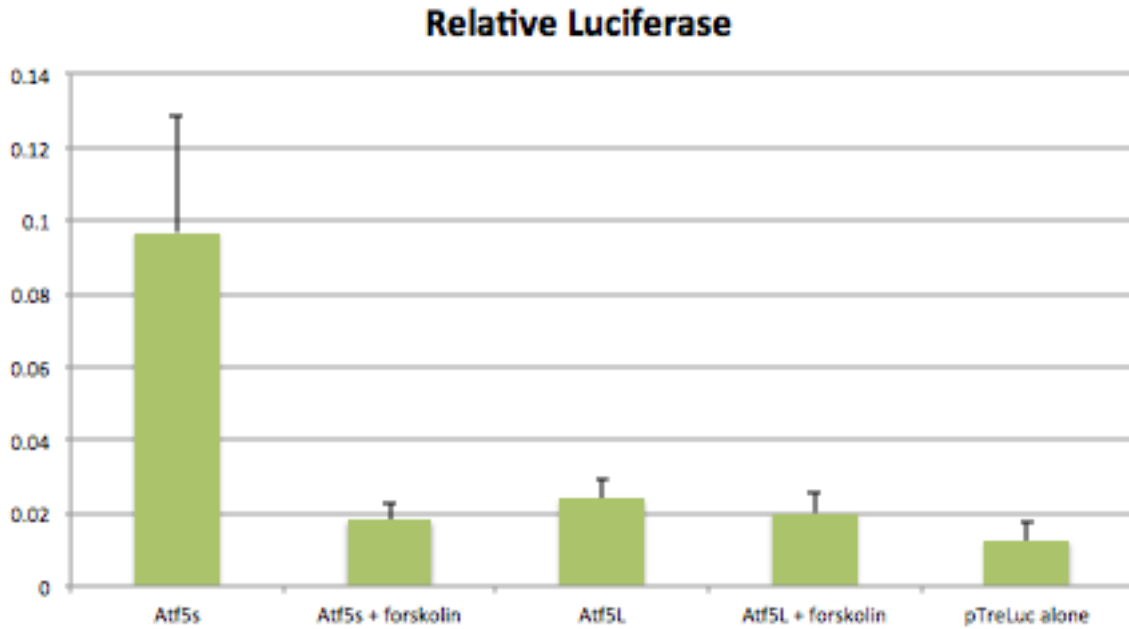


Figure 14: Relative luciferase signal from HEK cells transfected with Atf5s or Atf5L constructs with and without forskolin. Data shown are an average of three independent experiments, with bars representing standard error.

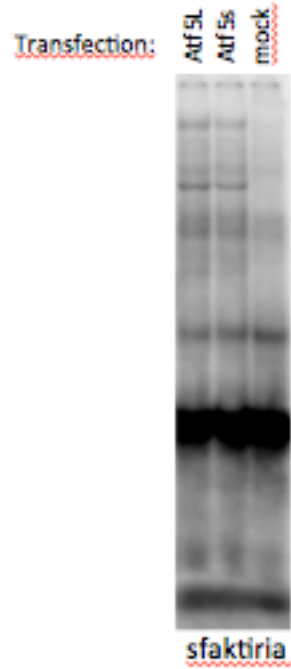


Figure 15: EMSA assay using radiolabeled probe derived from the OR enhancer Sfaktiria, incubated with either Atf5s-transfected cell lysate, Atf5L-transfected lysate, or mock-transfected cell lysate.

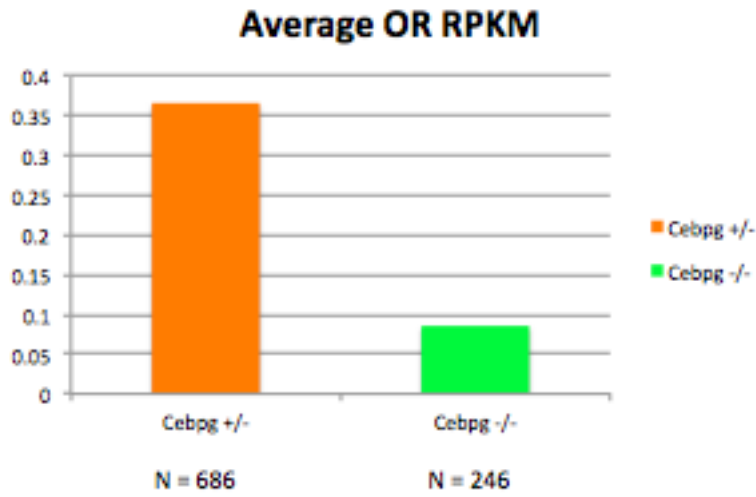


Figure 16: OR mRNA expression in P0 whole MOE from *Cebpg +/-* and *Cebpg -/-* animals. Shown are average OR RPKM and number of ORs detected.

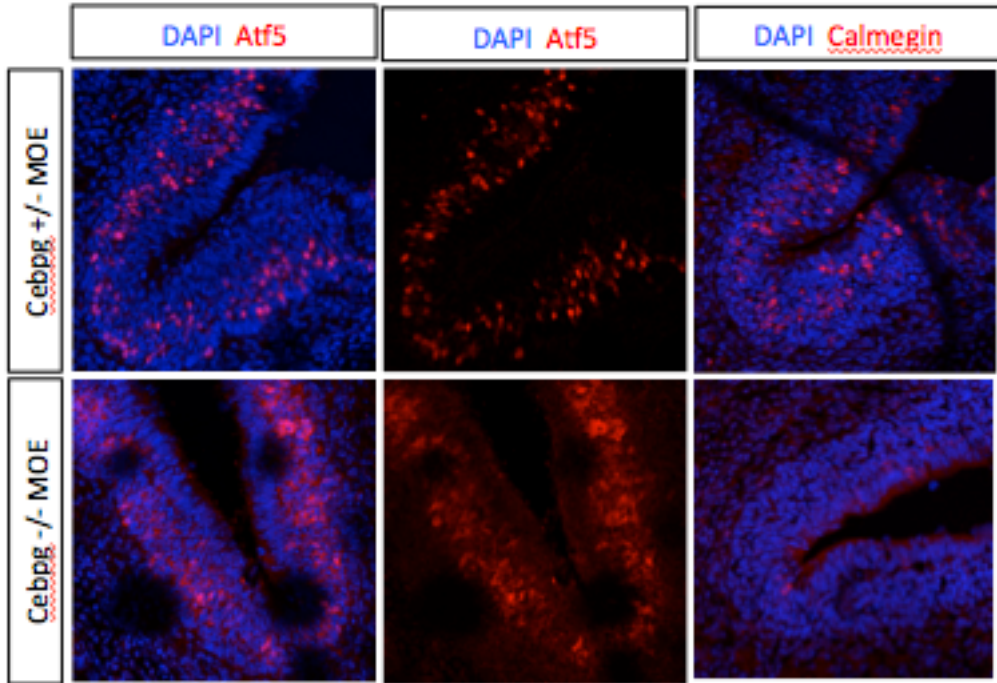


Figure 17: Atf5 and Calmegin protein expression in P0 Cebpg +/- and Cebpg -/- littermates.

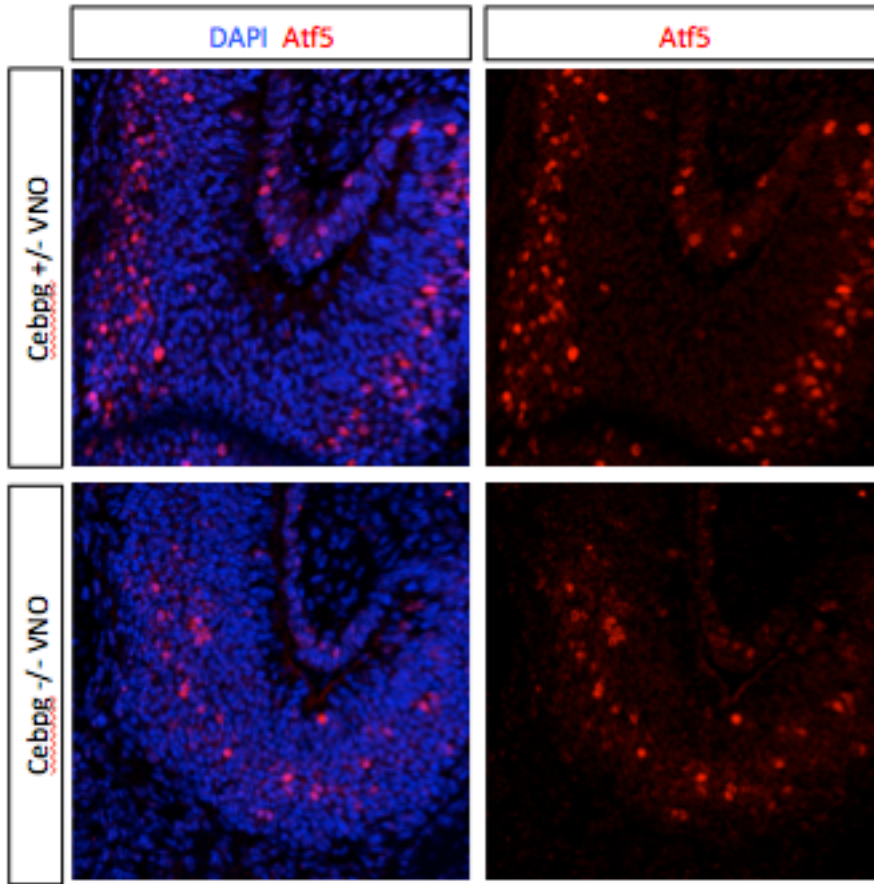


Figure 18: Atf5 protein expression in P0 VNO of Cebpg +/- and Cebpg -/- animals

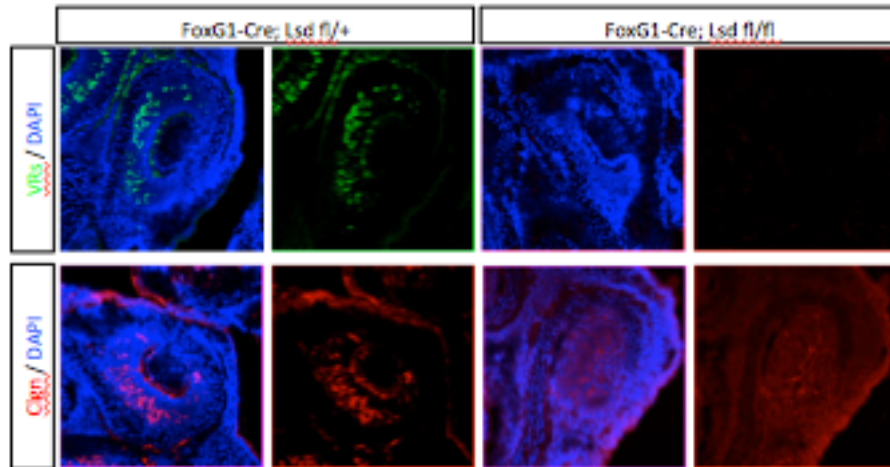


Figure 19: E18 Lsd1 mutant and control sections stained with a pool of VR antibodies or Calmegin antibody

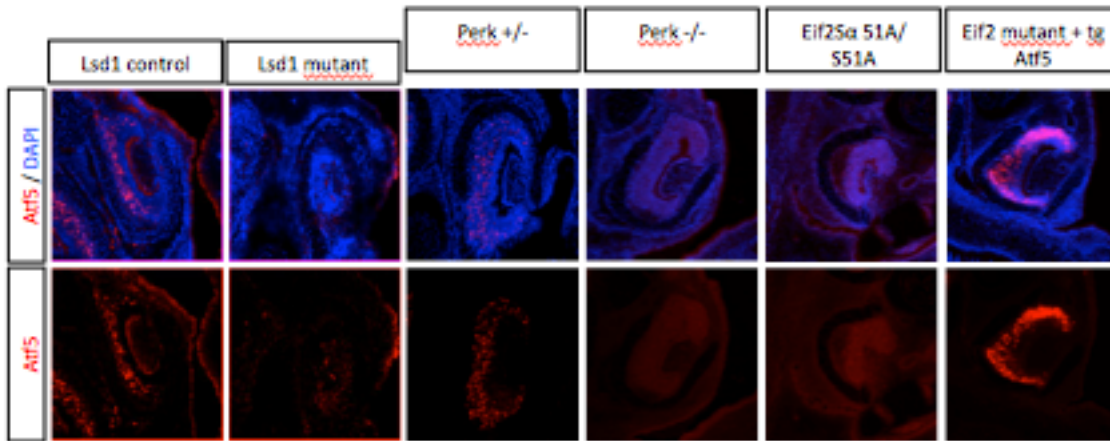


Figure 20: Atf5 protein expression in Lsd1 mutant, control, *Perk* +/-, *Perk* -/-, *Eif2S51A/S51A*, and *Eif2S51A/S51A*; Atf5 transgenic rescue animals

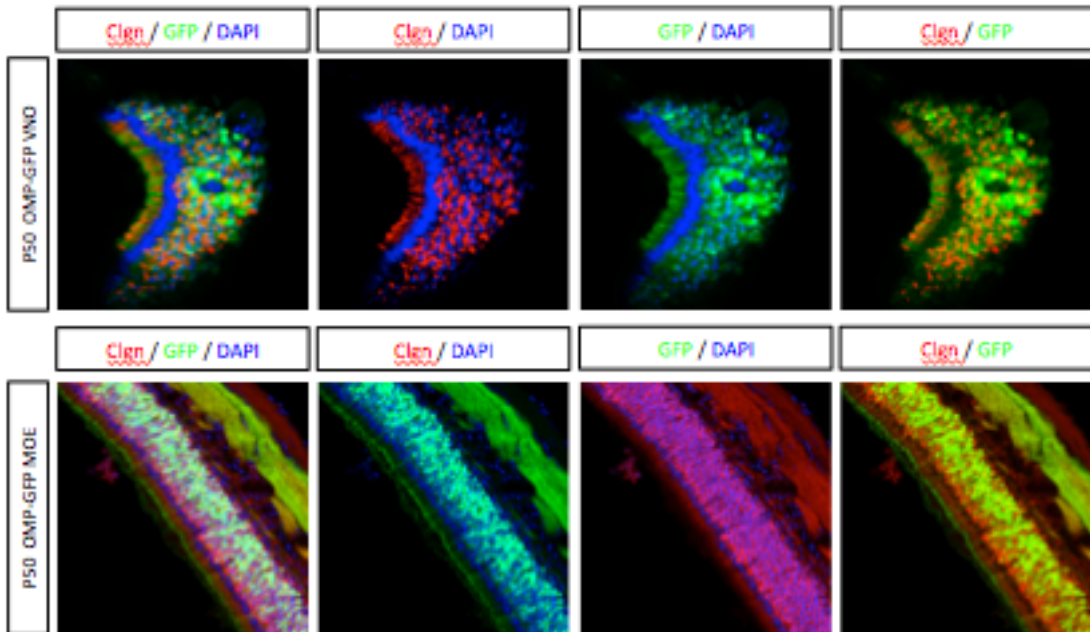


Figure 21: Clgn and OMP-GFP protein expression in P50 MOE and VNO

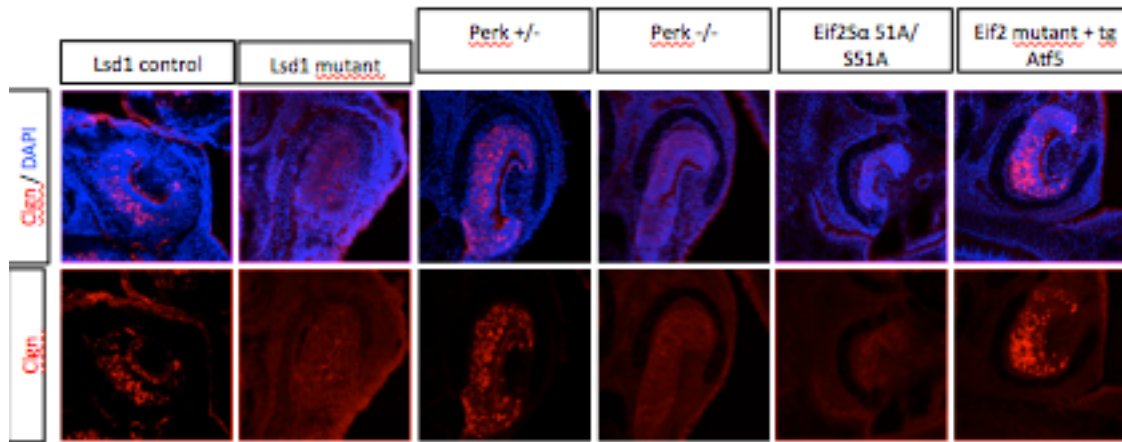


Figure 22: CLGN protein expression in Lsd1 mutant, control, *Perk* +/-, *Perk* -/-, *Eif2S51A/S51A*, and *Eif2S51A/S51A*; *Atf5* transgenic rescue animals

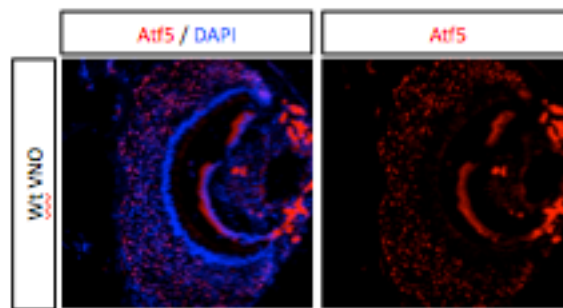
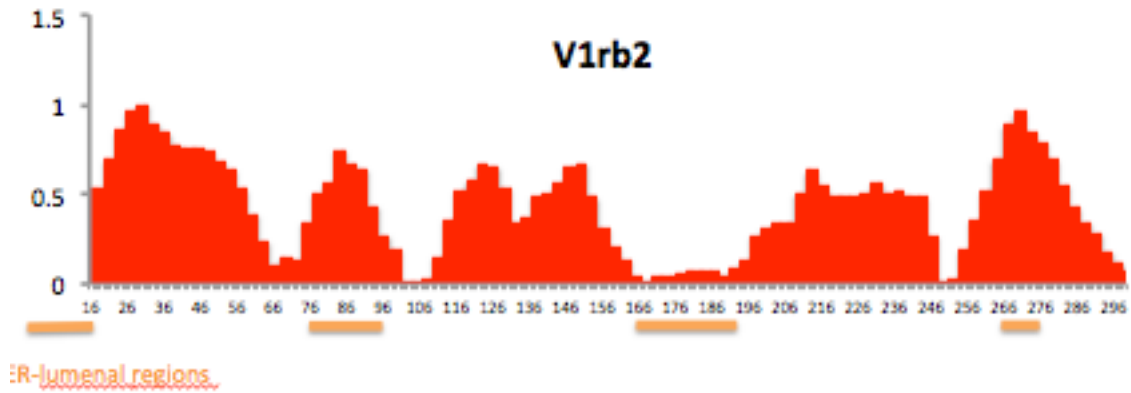


Figure 23: top: Peptide array data for V1rb2. Data shown as relative binding versus amino acid position. ER-luminal regions are highlighted in gold. Bottom: Atf5 protein expression in adult VNO.

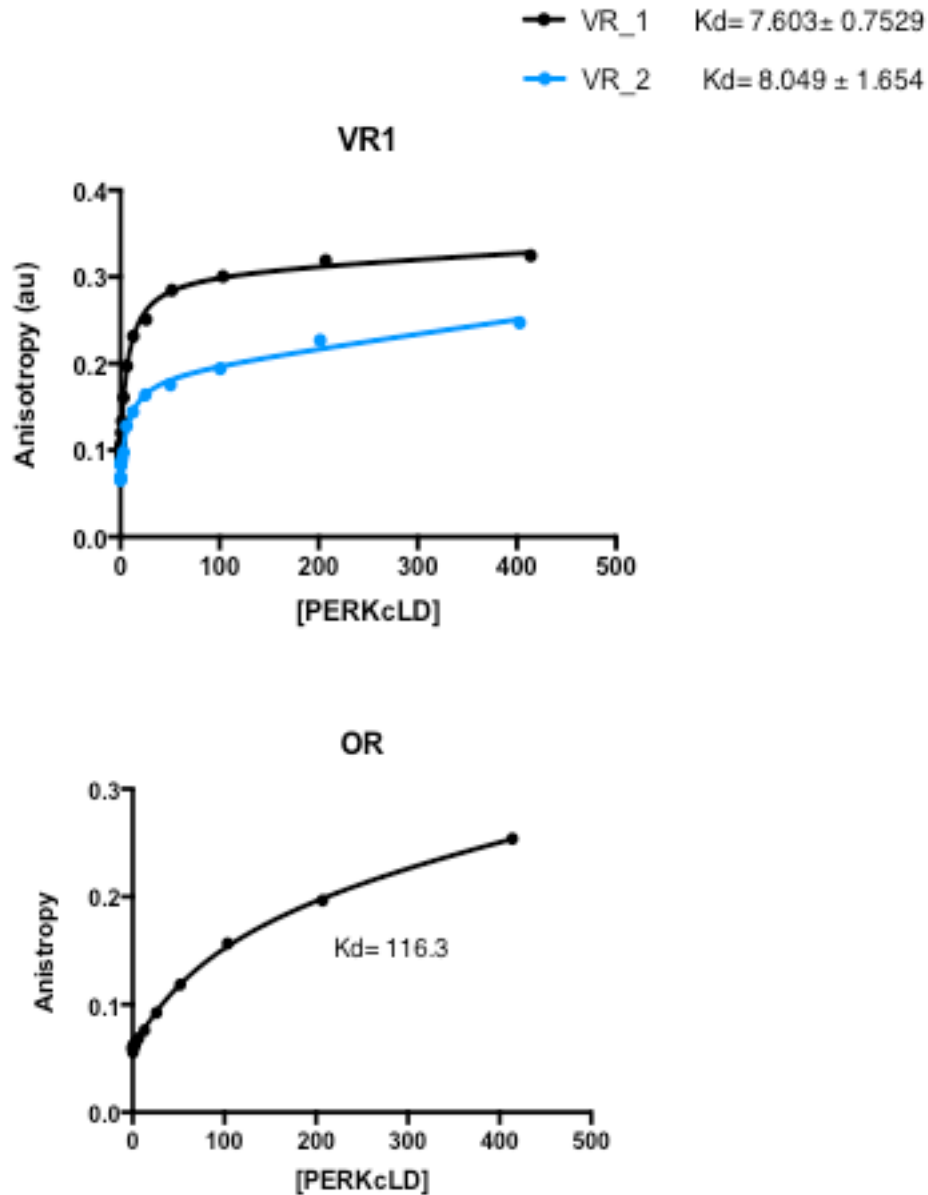


Figure 24: Fluorescence anisotropy experiments for peptides derived from the second and fourth ER-luminal regions of V1rb2 or the second ER-luminal region of Olfr1507. Data shown as arbitrary anisotropy units versus PERK cLD concentration

I. References

Araneda RC, Kini AD, Firestein S. 2000. The molecular receptive range of an odorant receptor. *Nat. Neurosci.* 12:1248-55

Barnea G, O'Donnell S, Mancina F, Sun X, Nemes A, et al. 2004. Odorant receptors on axon termini in the brain. *Science* 304:1468

Berghard A, Buck LB. 1996. Sensory transduction in vomeronasal neurons: evidence for G α o, G α i2, and adenylyl cyclase II as major components of a pheromone signaling cascade. *J. Neurosci.* 16:909-18

Bozza T, Vassalli A, Fuss S, Zhang JJ, Weiland B, et al. 2009. Mapping of class I and class II odorant receptors to glomerular domains by two distinct types of olfactory sensory neurons in the mouse. *Neuron* 61:220-33

Buck L, Axel R. 1991. A novel multigene family may encode odorant receptors: a molecular basis for odor recognition. *Cell* 65: 175-87.

Cau E, Gradwohl G, Fode C, Guillemot F. 1997. Mash1 activates a cascade of bHLH regulators in olfactory neuron progenitors. *Development* 124:1611-21.

Chess A, Simon I, Cedar H, Axel R. 1994. Allelic inactivation regulates olfactory receptor gene expression. *Cell* 100:703-11.

Clowney EJ, Magklara A, Colquitt BM, Pathak N, Lane RP, Lomvardas S. 2011. High-throughput mapping of the promoters of mouse olfactory receptor genes reveals a new type of mammalian promoter and provides insight into olfactory receptor gene regulation. *Genome Res.* 21:1249-59

Clowney EJ, Legros MA, Mosley CP, Clowney FG, Markenscoff-Papadimitriou EC, et al. 2012. Nuclear aggregation of olfactory receptor genes governs their monogenic expression. *Cell* 151:724-37

Del Punta K, Leinders-Zufall T, Rodriguez I, Jukam D, Wysocki C, et al. 2002. Deficient pheromone responses in mice lacking a cluster of vomeronasal receptor genes. *Nature* 419:70-74

Dulac C, Axel R. 1995. A novel family of genes encoding putative pheromone receptors in mammals. *Cell* 83:195-206

Ebrahimi F, Chess A. 2000. Olfactory neurons are interdependent in maintaining axonal projections. *Curr. Biol.* 10:219-22

Ferreira T, Wilson SR, Choi YG, Risso D, Dudoit S, et al. 2014. Silencing of odorant receptor genes by G protein $\beta\gamma$ signaling ensures the expression of one odorant receptor per olfactory sensory neuron. *Neuron* 81:847-859.

Feinstein P, Bozza T, Rodriguez I, Vassalli A, Mombaerts P. 2004. Axon guidance of mouse olfactory sensory neurons by odorant receptors and the B2 adrenergic receptor. *Cell* 117:833-46

Ferrero DM, Lemon JK, Fluegge D, Pashkovski S, Korzan WJ, et al. 2011. Detection and avoidance of a carnivore odor by prey. *PNAS* 108:11235-40

Ferrero DM, Wacker D, Roque M, Baldwin MQ, Stevens C, Liberles SD. 2012. Agonists for 13 trace amine-associated receptors provide insight into the molecular basis of odor selectivity. *ACS Chem. Biol.* 7:1184-89

Fuss SH, Omura M, Mombaerts P. 2007. Local and *cis* effects of the H element on expression of odorant receptor genes in mouse. *Cell* 130:373-84

Gardner B & Walter P. 2011. Unfolded proteins are Ire1-activating ligands that directly induce the unfolded protein response. *Science* 333:1891-94

Halpern M. 1987. The organization and function of the vomeronasal system. *Annu. Rev. Neurosci.* 10:325-62

Hansen MN, Mitchelmore C, Kjaerfulff KM, Rasmussen TE, Pedersen KM, Jensen NA. Mouse Atf5: molecular cloning of two novel mRNAs, genomic organization, and odorant sensory neuron localization. *Genomics* 80:344-50

Hirota J, Mombaerts P. 2004. The LIM-homeodomain protein Lhx2 is required for complete development of mouse olfactory sensory neurons. *PNAS* 101:8751-55

Hirota J, Omura M, Mombaerts P. 2007. Differential impact of Lhx2 deficiency on expression of class I and class II odorant receptor genes in mouse. *Mol. Cell Neurosci.* 34:679-88

Imai T, Suzuki M, Sakano H. 2006. Odorant receptor-derived cAMP signals direct axonal targeting. *Science* 314:657-661.

Ishii T, Hirota J, Mombaerts P. 2003. Combinatorial coexpression of neural and immune multigene families in mouse vomeronasal sensory neurons. *Curr. Biol.* 13:394-400

Ishii T, Mombaerts P. 2008. Expression of nonclassical class 1 major histocompatibility genes defines a tripartite organization of the mouse vomeronasal system. *J. Neurosci.* 28:2332-41

Ishii T, Mombaerts P. 2011. Coordinated coexpression of two vomeronasal receptor V2R genes per neuron in the mouse. *Mol. Cell. Neurosci.* 46:397-408

Johnson MA, Tsai L, Roy DS, Valenzuela DH, Mosley C, et al. 2012. Neurons expressing trace amine-associated receptors project to discrete glomeruli and constitute an olfactory subsystem. *PNAS* 109:13410-15

Jones DT, Masters SB, Bourne HR, Reed RR. 1990. Biochemical characterization of three stimulatory GTP-binding proteins: the large and small forms of Gs and the olfactory-specific G-protein, Golf. *J. Biol. Chem.* 265:2671-76

Khan M, Vaes E, Mombaerts P. 2011. Regulation of the probability of mouse odorant receptor gene choice. *Cell* 147:907-21

Lane RP, Cutforth T, Axel R, Hood L, Trask BJ. 2002. Sequence analysis of mouse vomeronasal receptor gene clusters reveals common promoter motifs and a history of recent expansion. *PNAS* 99:291-96

Liberles SD, Buck LB. 2006. A second class of chemosensory receptors in the olfactory epithelium. *PNAS* 103:645-50

Liberles SD, Horowitz LF, Kuang D, Contos JJ, Wilson KL, et al. 2009. Formyl peptide receptors are candidate chemosensory receptors in the vomeronasal organ. *PNAS* 106:9842-47

Lewcock JW, Reed RR. 2004. A feedback mechanism regulates monoallelic olfactory receptor expression. *PNAS* 101:1069-74

Leinders-Zufall T, Ishii T, Chaero P, Hendrix P, Oboti L, et al. 2014. A family of nonclassical class I MHC genes contributes to ultrasensitive chemodetection by mouse vomeronasal sensory neurons. *J. Neurosci* 34:5121-33

Levi G, Puche A, Mantero S, Barbien O, Trombino S, et al. 2003. The *Dlx5* homeodomain gene is essential for olfactory development and connectivity in the mouse. *Mol. Cell Neurosci.* 22:530-43

Levy NS, Bakalyar HA, Reed RR. 1991. Signal transduction in olfactory neurons. *J. Steroid Biochem. Mol Biol.* 39:633-37

Loconto J, Papes F, Chang E, Stowers L, Jones EP, et al. 2003. Functional expression of murine V2R pheromone receptors involves selective association with the M10 and M1 families of MHC class 1b molecules. *Cell* 112:607-18

Lomvardas S, Barnea G, Pisapia DJ, Mendelsohn M, Kirkland J, Axel R. 2006.

Interchromosomal interactions and olfactory receptor choice. *Cell* 126:403-13

Lyons DB, Allen WE, Goh T, Tsai L, Barnea G, Lomvardas S. 2013. An epigenetic trap stabilizes singular olfactory receptor choice. *Cell* 126:403-13

Lyons DB, Magklara A, Goh T, Sampath SC, Schaefer A, et al. 2014. Heterochromatin-mediated gene silencing facilitates the diversification of olfactory neurons. *Cell Rep.* 9:884-92

Magklara A, Yen A, Colquitt BM, Clowney EJ, Allen W, et al. 2011. An epigenetic signature for monoallelic olfactory receptor expression. *Cell* 145:555-70

Markenscoff-Papadimitriou E, Allen WE, Colquitt BM, Goh T, Murphy KT, et al. 2014. Enhancer interaction networks as a means for singular olfactory receptor expression. *Cell* 159:543-57

Martini S, Silvotti L, Shirazi A, Ryba NJ, Tirindelli R. 2001. Co-expression of putative pheromone receptors in the sensory neurons of the vomeronasal organ. *J. Neurosci.* 21:843-48

McIntyre JC, Bose SC, Stromberg AJ, McClintock TS. 2008. Emx2 stimulates odorant receptor gene expression. *Chem. Senses* 33:825-37

Michaloski JS, Galante PA, Malnic B. 2006. Identification of potential regulatory motifs in odorant receptor genes by analysis of promoter sequences. *Genome Res.* 16:1091-98

Michaloski JS, Galante PA, Nagai MH, Sakano H. 2005. Continuous and overlapping expression domains of odorant receptor genes in the olfactory epithelium determine the dorsal/ventral positioning of glomeruli in the olfactory bulb. *J. Neurosci.* 25:3586-92

Miyamichi K, Serizawa S, Kimura HM, Sakano H. 2005. Continuous and overlapping expression domains of odorant receptor genes in the olfactory epithelium determine the dorsal/ventral positioning of glomeruli in the olfactory bulb. *J. Neurosci.* 25:3586-92

Mombaerts P, Wang F, Dulac C, Chao S, Nemes M, et al. 1996. Visualizing an olfactory sensory map. *Cell* 87:675-86

Mombaerts P. 1999. Seven-transmembrane proteins as odorant and chemosensory receptors. *Science* 286:707-11

Neuhaus E, Mashukova A, Zhang W, Barbour J, & Hatt H. 2006. A specific heat shock protein enhances expression of mammalian olfactory receptor proteins. *Chem. Senses* 31:445-52

Plessy C, Pascarella G, Bertin N, Akalin A, Carrieri C, et al. 2012. Promoter architecture of mouse olfactory receptor genes. *Genome Res.* 22:486-97

Ressler HJ, Sullivan SL, Buck LB. 1994. Information coding in the olfactory system: evidence for a stereotyped and highly organized epitope map in the olfactory bulb. *Cell* 79:1245-55

Riviere S, Challet L, Fluegge D, Spehr M, Rodriguez I. 2009. Formyl peptide receptor-like proteins are a novel family of vomeronasal chemoreceptors. *Nature* 459:574-77

Rodriguez I, Feinstein P, Mombaerts P. 1999. Variable patterns of axonal projections of sensory neurons in the mouse vomeronasal system. *Cell* 97:199-208

Rodriguez-Gil D, Treolar HM, Zhang H, Miller AM, Two A, et al. 2010. Chromosomal location-dependent nonstochastic onset of odorant receptor expression. *J. Neurosci.* 30:10067-75

Ron D, Walter P. 2007. Signal integration in the endoplasmic reticulum unfolded protein response. *Nat. Rev. Mol. Cell Biol.* 8:519-29

Roppolo D, Vollery S, Kan CD, Luscher C, Broiller MC, Rodriguez I. 2007. Gene cluster lock after pheromone receptor gene choice. *EMBO J.* 26:3423-30

Ryba NJ, Tirindelli R. 1997. A new multigene family of putative pheromone receptors. *Neuron* 19:371-79

Saito H, Kubota M, Roberts RQ, Chi Q, Matsunami H. 2004. RTP family members induce functional expression of mammalian odorant receptors. *Cell* 119:679-91

Serizawa S, Kazunari M, Nakatani H, Suzuki M, Saito M, et al. 2003. Negative Feedback Regulation Ensures the One Receptor-One Olfactory Neuron Rule in Mouse. *Science* 302:2088-94

Sullivan SL, Adamson MC, Ressler KJ, Kozak CA, Buck LB. 1996. The chromosomal distribution of mouse odorant receptor genes. *PNAS* 93: 884-88.

Vassalli A, Rothman A, Feinstein P, Zapotocky M, Mombaerts P. 2002. Minigenes impart odorant receptor-specific axon guidance in the olfactory bulb. *Neuron* 35:681-96

Vassar R, Chao SK, Sitcheran R, Nunez JM, Vosshall LB, Axel R. 1994. Topographic organization of sensory projections to the olfactory bulb. *Cell* 79:981-91

Vassar R, Ngai J, Axel R. 1993. Spatial segregation of odorant receptor expression in the mammalian olfactory epithelium. *Cell* 74:309-18

Vatter K & Wek R. 2004. Reinitiation involving upstream ORFs regulates *ATF4* mRNA translation in mammalian cells. *PNAS* 101:11269-74

Wang F, Nemes A, Mendelsohn M, Axel R. 1998. Odorant receptors govern the formation of a precise topographic map. *Cell* 93:47-60

Wang SZ, Ou J, Zhu LJ, Green MR. 2012. Transcription factor ATF5 is required for terminal differentiation and survival of olfactory sensory neurons. *PNAS* 109:18589-94

Watatani Y, Ichikawa K, Nakanishi N, Fujimoto M, Takeda H, et al. 2008. Stress-induced translation of ATF5 mRNA is regulated by the 5'-untranslated region. *J. Biol. Chem.* 283:2543-53

Wu L, Pan Y, Chen GQ, Matsunami H, Zhuang H. 2012. Receptor-transporting protein 1 short (RTP1S) mediates translocation and activation of odorant receptors by acting through multiple steps. *J. Biol. Chem.* 287:22287-94

Zhang X, Firestein S. 2002. The olfactory receptor gene superfamily of the mouse.
Nat. Neurosci. 5:124-33.

Publishing Agreement

It is the policy of the University to encourage the distribution of all theses, dissertations, and manuscripts. Copies of all UCSF theses, dissertations, and manuscripts will be routed to the library via the Graduate Division. The library will make all theses, dissertations, and manuscripts accessible to the public and will preserve these to the best of their abilities, in perpetuity.

Please sign the following statement:

I hereby grant permission to the Graduate Division of the University of California, San Francisco to release copies of my thesis, dissertation, or manuscript to the Campus Library to provide access and preservation, in whole or in part, in perpetuity.



Author Signature



Date